# Innate cGAS-STING Signaling in Doxorubicin Cardiomyopathy.

By

Raneeta Thingnam

A Thesis submitted to the Faculty of Graduate Studies of
The University of Manitoba
in partial fulfilment of the requirements of the degree of

MASTER OF SCIENCE

Department of Physiology and Pathophysiology
University of Manitoba
Winnipeg

**Abstract**

**Introduction:** Doxorubicin (DOX) is widely used to treat a variety of human cancers. However, a well-known but poorly understood side effect of DOX treatment is its cardiotoxic properties, which trigger cardiac cell death and heart failure. Autophagy is a cellular process responsible for the removal and degradation of damaged cellular components and proteins through a lysosomal regulated pathway. Previous research demonstrated that autophagy is impaired in cancer patients and mice treated with DOX. The cyclic GMP-AMP synthase (cGAS) - stimulator of interferon genes STING (cGAS-STING), is part of the innate immunity signaling pathway activated by cellular DAMPs such as nuclear DNA and chromatin associated HMBG1. Activation of cGAS-STING leads to cytokine production and cell death. However, the involvement of cGAS – STING pathway in DOX-cardiomyopathy is not well understood. Herein, we investigated the role of cGAS-STING pathway in DOX-induced cardiotoxicity, as well as explore potential therapeutic interventions.

**Methods:** Neonatal cardiac myocytes (NCMCs) were isolated from 1-2 days old Sprague-Dawley rats and were treated with DOX in increasing doses (0.5μM, 1μM, 2.5μM, 5μM and 10μM). After eighteen hours of treatment, the cells were processed for Western blot analysis to evaluate the protein expression of protein markers involved in the innate immune pathway. To assess the impact of cGAS and STING inhibition on DOX-induced toxicity, cell viability and mitochondrial function assays were performed in presence and absence of the inhibitors on DOX treated cardiomyocytes.

**Results and conclusion:** Our findings demonstrate that in contrast to vehicle treated cells, DNA is present in the cytosol of cardiac myocytes when treated with DOX. This coincided with activation of cGAS-STING pathway, accompanied by elevated expression of NLRP3 and Bnip3 proteins leading to wide spread cell death. Notably, pharmacologic inhibition of cGAS or STING independently suppressed DOX-induced cardiac cell death. Our data reveal for the

first time the involvement of cGAS-STING innate signaling pathway in the pathogenesis of DOX cardiotoxicity. We suggest that therapeutic interventions that modulate the innate immune pathway may prove beneficial to preserving cardiac function and mitigating cardiotoxicity in cancer patients treated with Dox.

**Acknowledgement**

I would like to express my deepest gratitude to my supervisor, Dr. Lorrie Kirshenbaum, for his invaluable guidance, mentorship, and unwavering support throughout my research journey. His expertise and insightful feedback have been instrumental in shaping my work and fostering my growth as a researcher. Beyond the lab, Dr. Kirshenbaum has continually inspired me to pursue opportunities that extend beyond academic research. It has been an incredible experience to see a scientific idea come to life under his mentorship. For all of this and more, I am truly thankful.

I would also like to extend my sincere thanks to my committee members, Dr. Sanjiv Dhingra and Dr. Inna Rabinovich-Niktin, for their helpful feedback and expertise throughout my research. Their constructive insights have greatly enhanced the quality of my work and enriched my academic experience.

A special acknowledgment goes to the Kirshenbaum Lab. I am deeply grateful to have been part of such an exceptional group of individuals who have created such a supportive and collaborative research environment. I would like to thank Dr. Rimpy Dhingra for generously sharing her expertise with me, and guiding me through the challenges I encountered during my research journey. To Victoria Margulets, thank you for your assistance with cell culture and microscopy and for sharing your genuine excitement for science. I am also grateful to Floribeth Aguilar for her guidance with laboratory techniques and her constant support. Thank you Ms. Kairee Ryplanski and Ms. Mae Villamor, for their help with administrative tasks, which eased many aspects of my work and allowed me to focus on my research goals. I would also like to acknowledge Molly Crandall, Darya Nematisouldaragh, Dr. Sukhwinder Bhullar, Amit Suharenko, and Ben Margulets for their support and being helpful lab members. Being part of this lab has been an enriching experience that I will always cherish.

On a personal note, I am forever grateful to my parents for their unwavering support and encouragement throughout this journey. Thank you, Dad, for inspiring me to pursue a career in research and always believing in me. Thank you, Mom, for pushing me to prioritize education. I would also like to thank my brother, Rayvin, for cheering me on every step of the way.

Finally, I extend my heartfelt thanks to my friends - Anandita, for your continuous trust and belief in me; Ananya, for your chaotic sleep schedule and for always being a willing listener despite the time-zone difference; Can, for being an incredible friend and helping me adjust to a new country (also for sending me photos of your cats); Rubal, for your constant support and friendship, and Vibhuti di, for your encouragement to always aim higher. Thank you all, and many others, for making this journey a little less tiring.

This journey has been an immense learning experience, on both a professional and personal level. It would not have been possible without the incredible support system around me. Thank you all for making this experience so meaningful!

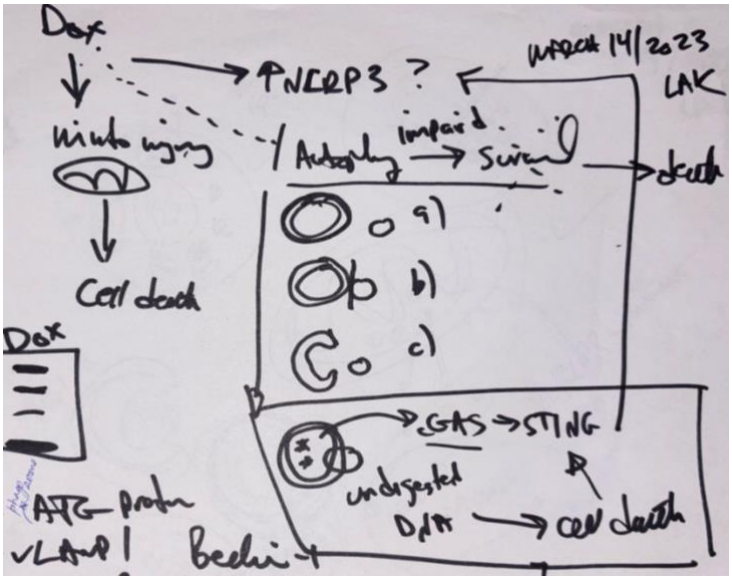


Image 1 : First teaching lesson with Dr. Kirshenbaum

# Table of Contents

**List of Figures**

**List of Abbreviations**

| | |
|---|---|
| ΔΨm | Mitochondrial membrane potential |
| AAD | Aortic aneurysm and dissection |
| AIF | Apoptosis-inducing factor |
| AIM2 | Absent in Melanoma 2 |
| AngII | Angiotensin II |
| ATP | Adenosine triphosphate |
| BNIP3 | Bcl-2 19-kD interacting protein 3 |
| Ca2+ | Calcium |
| cGAS | Cyclic GMP-AMP synthase |
| cGAMP | Cyclic guanosine monophosphate (GMP) – adenosine monophosphate (AMP) |
| CHF | Congestive heart failure |
| cTnT | Cardiac troponin T |
| CVDs | Cardiovascular diseases |
| DAMPs | Damage-associated molecular patterns |
| DNA | Deoxyribonucleic acid |
| DOX | Doxorubicin |
| DRP-1 | Dynamin-related protein 1 |
| dsDNA | Double stranded DNA |
| ECG | Electrocardiogram |
| EndoG | Endonuclease G |
| ER | Endoplasmic reticulum |
| GFP | Green fluorescent protein |
| GSDMD | Gasdermin D |
| GTP | Guanosine Triphosphate |

| | |
|---|---|
| HMGB-1 | High-mobility G box protein 1 |
| IFN3 | IFN regulatory factor-3 |
| IL | Interleukins |
| IRI | Ischemia reperfusion injury |
| LDH | Lactate dehydrogenase |
| LVEF | Left ventricular ejection fraction |
| MFN | Mitofusin |
| mPTP | Mitochondrial permeability transition pore |
| mtDNA | Mitochondrial DNA |
| NADPH | Nicotinamide adenine dinucleotide phosphate |
| Ncf1 | Neutrophil cytoplasmic factor 1 |
| NCMCs | Neonatal cardiac myocytes |
| NF-κB | Nuclear factor-kappa B |
| NLRs | Nod-like receptors |
| NLRP3 | NOD-like receptor protein 3 |
| NOS | Nitric oxide synthase |
| NOX | NADPH oxidase |
| Nrf2 | Nuclear factor erythroid 2-related factor 2 |
| PAMPs | Pathogen-associated molecular patterns |
| PRRs | Pattern recognition receptors |
| ROS | Reactive oxygen species |
| SERCA | Sarcoplasmic reticulum calcium-ATPase |
| SLE | Systemic lupus erythematosus |
| SMC | Smooth muscle cells |
| SR | Sarcoplasmic reticulum |

| | |
|---|---|
| STING | Stimulator of interferon genes |
| TBK-1 | TANK binding kinase-1 |
| TLRs | Toll-like receptors |
| TNFα | Tumor necrosis factor-α |
| TopII | Topoisomerase II |
| TRAF2 | TNF receptor associated factor 2 |

## Introduction

Anthracycline drugs, particularly Doxorubicin (DOX), are widely employed as a first-line treatment strategy for a broad spectrum of human cancers due to its highly potent anti-cancer properties (1,2). Despite its strong efficacy against cancer, DOX's well-known yet poorly understood side effect is that it can induce severe cardiac damage. Notably, in some cases, the chemotherapy has to be stopped because the cardiotoxic effects of DOX are life threatening. Hence, as a result cancer patients go without the required anti-cancer treatment (3). The cardiovascular complications associated with DOX manifest in a dose-dependent manner either acutely, within a few days of initiation of therapy or chronically, occurring several decades after treatment has been discontinued (4). In severe cases, the prognosis following DOX therapy is poor and often manifests as heart failure, which is the leading cause of mortality among cancer survivors (3).

Autophagy is a cellular process responsible for degrading and recycling damaged cellular components and proteins. The process entails the sequestration of damaged or dysfunctional components through the formation of specialized structures called autophagosomes. Subsequently, when autophagosomes fuse with lysosomes to form autolysosomes, the autophagosome cargo is degraded by the action of lysosomal enzymes. Therefore, autophagy is essential for maintaining cellular homeostasis and promoting cell survival (5). Under normal conditions, autophagy serves as a cytoprotective mechanism, mitigating cardiac damage and cell death by eliminating ROS (reactive oxygen species) producing mitochondria and clearing cellular debris (6). Previous research, including studies from our laboratory, suggests that DOX causes mitochondrial dysfunction and necrotic cell death of cardiomyocytes mediated by Bnip3 (Bcl-2 19-kD interacting protein) activity (7). Additionally, it has been reported that DOX

inhibits autophagic flux (5) leading to accumulation of cellular debris and damaged organelles such as mitochondria. Thereby contributing to DOX-induced pathology.

Elevation in the release of inflammatory cytokines has been linked to DOX-induced cardiotoxicity (8). Studies have shown that, in cardiac myocytes treated with DOX there is a marked increase in the levels of inflammatory cytokines such as TNF-α , loss of nuclear-associated high-mobility G box protein 1 (HMGB-1) and DNA damage (9,10). Since DOX impairs autophagy, several damaged organelles and proteins such as mitochondria, HMGB-1 and DNA escape lysosomal digestion and accumulate in the cytosol (11). HMGB-1 and DNA can activate the innate immune signaling as a damage-associated molecular pattern (DAMP) response. Thereby triggering the cyclic GMP-AMP (cGAMP) synthase (cGAS) stimulator of interferon genes (STING) (cGAS-STING) pathway resulting in the activation of interferons and cell death (7). cGAS is a DNA sensor and binding with cytosolic DNA causes its activation, which leads to the synthesis of cGAMP from GMP and ATP. cGAMP acts as a secondary messenger and has a high affinity for STING, which is localised on the endoplasmic reticulum (ER). Binding of cGAMP to STING leads to its subsequent activation. This promotes STING stimulated release of pro-inflammatory cytokines such as type 1 interferons via TANK binding kinase-1 (TBK-1) and IFN regulatory factor-3 (IFN3) molecular pathway (12).

Abnormal activation of cGAS – STING pathway and inflammation is intricately linked with cardiovascular disorders such as myocardial infarction and aortic aneurysm and dissection (13,14). However, the involvement of cGAS – STING pathway needs more investigation in regards to DOX-induced cardiomyopathy. The primary focus of this project will be to elucidate the role of the innate immune signaling cGAS-STING pathway response in the pathogenesis of DOX cardiomyopathy.

Doxorubicin has been part of treatment strategies for human cancer since the 1960s and is still the most commonly and widely used chemotherapy drug (3,15). Nonetheless, cardiomyopathy induced by DOX remains a major challenge and risk factor for cancer patients developing heart failure while undergoing DOX treatment. Further, the involvement of innate signaling pathway in DOX cardiotoxicity is untested. Hence, understanding the molecular mechanisms that underlie DOX-induced cardiomyopathy is of great scientific and clinical importance for developing new treatment strategies to improve cancer patient care.

## Literature Review

### 1. Doxorubicin in Cancer Treatment :

Doxorubicin (DOX) is an anthracycline drug isolated from *Streptomyces peucetius var. caesius* in the 1960s (16). Being highly potent against cancer, it soon became one of the mainline therapies used for treating various human cancers. DOX is typically administered intravenously, either alone or in combination with other chemotherapy drugs, to treat breast cancer, sarcomas and acute leukaemia among others (17,18). The average dose of DOX varies depending on the specific type of cancer type, patient characteristics, and treatment protocol. However, a typical dose range for doxorubicin is 60-75 mg/m² of body surface area, administered every 21 days (19). DOX is a type of topoisomerase II (TopII) inhibitor that blocks the action of the topoisomerase enzyme that is responsible for regulating DNA replication and transcription. DOX intercalates itself into the DNA strand, leading to DNA breaks thus preventing replication (20).

Despite being a very effective chemotherapy drug, its cardiotoxic side effect is currently a major limitation in its clinical application.

### 2. Doxorubicin induced-cardiotoxicity :

DOX-induced cardiomyopathy can be manifested acutely or chronically depending on when the symptoms first manifest. The risk of manifesting cardiovascular side effects as a result of DOX treatment has a dose dependent relationship (21,22). The incidence of developing toxicity as a side effect is about 36% with a cumulative dose exceeding 600 mg/m2 (3). In a clinical trial involving a cohort of 630 patients randomized to receive doxorubicin plus placebo across three Phase III studies, 32 patients were diagnosed with congestive heart failure (CHF), indicating that approximately 26% of patients may experience doxorubicin-related CHF at a

cumulative dose of 550 mg/m² (21). The symptoms can manifest as reduction in left ventricular ejection fraction, arrhythmias, neutropenia and cardiac dysfunction (15). In severe cases of toxicity and poor prognosis, the patient can develop of end-stage CHF in which cardiac transplant becomes the last life-saving intervention for these patients (3). However, cardiac transplant comes with its own complex issue of the availability of donor hearts and the likelihood of cancer recurrence. Currently, dexrazoxane is the only US Food and Drug Administration approved drug that is used clinically prevent cardiac damage caused by DOX (23,24). Dexrazoxane is a strong iron chelating agent and is cardioprotective as it removes iron, reducing free radical formation in cardiac myocytes (25). The implication of dexrazoxane role in preventing cardiac damage induced by DOX is highly debatable. Where some studies show that dexrazoxane reduces the risk of cardiac dysfunction clinically in breast cancer patients undergoing anthracycline chemotherapy (26), others show that dexrazoxane has been statistically linked to reduced anti-cancer properties of DOX, increased haematological toxicity and increased risk of second malignant neoplasms (27,28). Therefore, investigation of adjuvant therapies which can prevent cardiomyopathy without compromising the anti-cancer effect of DOX is necessary.

## 3. Mechanisms of Doxorubicin cardiomyopathy :

Although the cardiotoxic side effect of DOX is well known it's still poorly understood. Research has shown that the mechanism involving dox induced cardiotoxicity is multifactorial. The proposed mechanisms that have gained attention have been described as follows.

### 3.1 Oxidative stress and ROS production :

Cardiomyocytes have the highest number of mitochondria compared to other tissue and cell types (29). This makes cardiac cells susceptible to DOX induced damage as DOX interacts

with the inner layer of mitochondria resulting in high production of reactive oxygen species (ROS) in the electron transport chain, leading to disrupted ATP synthesis and oxidative stress (30). Oxidative stress is caused by the imbalance in levels of ROS and antioxidants that can elicit cellular injury, triggering mitochondrial damage and cardiac dysfunction (30,31). Free radical overproduction can take place due to multiple processes such as redox cycling, nitric oxide synthase (NOS) uncoupling, interaction with NADPH oxidases (NOXs), and impaired mitochondrial respiration (31,32).

3.2 DNA damage :

The very property of DOX that makes it a chemotherapy drug can result in DNA damage in cardiomyocytes. As mentioned before, DOX is a topoisomerase II inhibitor (20). Topoisomerase has two isoforms topoisomerase II alpha (TOP2A) and topoisomerase II beta (TOP2B) (33). DOX binds to TOP2A in cancer cells and blocks the enzyme topoisomerase II, which results in a break in the DNA strand, as relaxation of supercoils in DNA are inhibited (34). However, TOP2A is not present in cardiomyocytes. Although DOX induces a similar reaction by binding to TOP2B, which is expressed in cardiac myocytes cause break in the double stranded DNA, affecting the transcription within mitochondrial DNA (mtDNA) and nuclear genomic DNA, resulting in cell death and cardiac dysfunction (33).

3.3 Impaired calcium homeostasis and contractile dysfunction :

The contractility of cardiac myocytes depends on the intracellular calcium concentration (35). DOX is associated with disruption in homeostasis of calcium flux resulting in contractile dysfunction and heart failure (33). In cardiac myocytes sarcoplasmic reticulum (SR) releases $Ca^{2+}$ to commence the contraction process. Studies have shown that DOX is involved in disruption of $Ca^{2+}$ uptake by sarcoplasmic reticulum $Ca^{2+}$-ATPase (SERCA) and reducing the

intracellular $Ca^{2+}$ transient amplitude. Additionally, DOX induces an elevation in diastolic $[Ca^{2+}]_I$, which impairs the function of the left ventricle (LV). Mitochondrial capacity of storing calcium is also strongly affected by DOX, causing calcium overload and mitochondrial dysfunction resulting in apoptotic cell death. This happens because DOX selective activates cyclosporin A-sensitive $Ca^{2+}$ channels in the mitochondria (36). Furthermore, ROS overproduction by DOX is closely linked to an increase in $Ca^{2+}$ as by pretreatment of the SR Ca2+ channel blockers and the antioxidants, ROS production was shown to be decreased (37).

3.4 Mitochondrial defects :

Cardiac myocytes are rich in mitochondria to meet the high energy requirement of the heart. Hence, the maintenance of mitochondrial integrity and functionality is crucial for proper cardiac function (38,39). The quality of mitochondria is maintained by mitochondrial proteostatics, mitochondrial biosynthesis, mitochondrial dynamics, mitochondrial DNA (mtDNA) repair and mitochondrial autophagy (40,41). Targeting of the mitochondria by DOX plays a significant role in cardiotoxicity induced by it (42). DOX accumulates in the mitochondria and disrupts the mitochondrial respiratory chain (7,43). It also stimulates the release of cytochrome C promoting apoptosis (44). Previous work from our laboratory has shown that BH3-only protein Bcl-2-like 19kDa-interacting protein 3 (Bnip3) which is part of the Bcl-2 family and is a mitochondrial death protein, mitigates DOX-induced necrosis in cardiomyocytes (7). Activation of Bnip3 provokes mitochondrial perturbation in the form of loss in mitochondrial membrane potential ($\Delta\Psi m$) and permeability transition pore (mPTP) opening (45). The study demonstrated that in $Bnip3^{-/-}$ mice were relatively resistant towards DOX-induced cardiotoxicity (7). Mitophagy homeostasis is important for maintaining mitochondrial health and recycling damaged mitochondria. However, studies have demonstrated that there is dysregulation of PINK1/Parkin-mediated mitophagy in the case of

DOX (46,47). An essential protein for mediating mitochondrial bioenergetics and mitochondrial fusion is Mitofusin 1 and Mitofusin 2(MFN1/2) (48). Meanwhile, dynamin-related protein 1 (DRP-1) controls mitochondrial fission (49). The imbalance between mitochondrial - fusion and fission has been linked to pathologies. MFN2 gets proteasomal degraded and DRP-1 is expressed at an elevated level in response to DOX and research have shown that targeting MFN2 and DRP-1 helps reduce mitochondrial perturbations and cell death induced by DOX (50,51). The ultrastructure defects in mitochondria induced by DOX alter the much-required ATP production for the proper functioning of cardiomyocytes (52,53). Additionally, elevated oxidative stress induced by DOX results in mitochondrial dysfunction and damage (30).

**4. Doxorubicin's effect on cell fate :**

The ultimate outcome of cellular damage of cardiomyocytes caused by DOX is cell death. Though the molecular pathogenesis remains unclear, DOX induces cell death via processes such as apoptosis, autophagy, ferroptosis, necrosis and pyroptosis. These pathways have been associated with acute DOX cardiomyopathy (54).

4.1 Apoptosis :

Programmed Cell Death (Apoptosis) induced by DOX can occur due to activation of both intrinsic (mitochondrial) and extrinsic (receptor-mediated) pathways. DOX treatment results in excessive ROS production and mitochondrial damage in cardiac myocytes which results in apoptotic cell death (55). Intrinsic apoptotic death of cardiomyocytes occurs as pro-apoptotic factors such as endonuclease G (EndoG), cytochrome c, and apoptosis-inducing factor (AIF) are released in the cytosol due to loss in mitochondrial membrane potential, mitochondrial swelling and outer membrane rupture (55). Bcl-2 family proteins play an important role in

regulating programmed cell death in mitochondria (56). DOX-induced cellular stress activates Bax/Bak translocation from the cytosol to the mitochondrial outer membrane, increasing membrane permeability and allowing the release of inner membrane proteins like cytochrome c (55). Presence of cytochrome c in the cytosol activates caspase resulting in cell death (57). Doxorubicin-induced DNA damage activates p53 which upregulates BAX expression, compromising mitochondrial membrane potential and promoting cell death, Notably, inhibition of p53 has been shown to attenuate these detrimental effects (58).

The extrinsic pathway is triggered when death ligands like FasL and TNF-α bind to their receptors, recruiting adaptor proteins Fas-associated via death domain (FADD) and TNFR-associated death domain (TRADD) (55,59). This results in caspase 8 and 3 activation causing cell death (57).

4.2 Autophagy :

Autophagy is a cellular process crucial for maintaining homeostasis by the clearance of damaged cellular organelles and proteins. Hence, this cellular clearance mechanism is vital for preserving cardiac structure and function under normal physiological conditions (60). Upregulation of autophagy serves as a protective response against various stressors in order to restrict damage and promote survival (60). Autophagy promotes cellular survival through catabolism, but dysfunctional autophagic activity can lead to cell death, potentially through necrosis and inflammation (61). Whether doxorubicin induces or disrupts autophagy in cardiac tissue is controversial as studies examining the role of autophagy in DIC have reported conflicting evidence (57). A study shows that inducing autophagy by rapamycin before DOX treatment increase cardiac cell survival as it reduces ROS production, apoptosis and improves mitochondrial function (62). Meanwhile, suppressing ATG7, a key regulator of autophagy, has been shown to mitigate doxorubicin-induced cardiotoxicity in both cell culture experiments

and chronic mouse models (63). Recent research has clarified these contradictory findings by suggesting that DOX initially stimulates the autophagy process but later inhibits its completion. This leads to the accumulation of undegraded autophagosomes and autolysosomes, which exacerbates cellular damage and ultimately contributes to the death of cardiomyocytes (11). DOX promotes the expression of LC3-II, p62 and Beclin1, thereby stimulating the beginning of autophagy (11). Conversely, DOX blocks the latter stages of the process by blocking autophagic flux and lysosomal acidification in cardiac myocytes. This disruption leads to the accumulation of autolysosomes, which in turn causes oxidative stress and contributes to cardiomyopathy (11,57).

4.3 Ferroptosis :

Introduced as a non-apoptotic mode of cell death in 2012, ferroptosis is an iron-dependant regulated cell death pathway involving the accumulation of iron and increased lipid peroxidation (64). As DOX intercalates itself in the mitochondrial DNA (mtDNA), it causes iron overload in the mitochondria, thereby inducing ferroptosis (65). A study demonstrated that by using ferrostatin 1 (Fer-1) a ferroptosis inhibitor, DOX-induced cardiomyopathic effects can be alleviated (66). Additionally, nuclear factor erythroid 2-related factor 2 (Nrf2) activation has also been used to suppress DOX-induced cardiomyocyte ferroptosis (67). Understanding of the molecular mechanism of DOX induced ferroptosis isn’t fully understood and is still developing.

4.4 Necrosis :

Acute form of DOX-induced cardiotoxicity involves necrotic cell death, which is characterised by cellular swelling resulting in cell bursting and leakage of cellular content in the environment, spreading inflammation to adjacent cells (52). Necrotic cell death of cardiomyocytes has been

tied to the activation of Bnip3 due to DOX (7). Cardiac myocytes treated with DOX have mitochondrial dysfunction, loss of nuclear HMGB1 and release of lactic acid dehydrogenase (LDH) and cardiac troponin T (cTnT), which serve as necrotic markers (7).

4.5 Pyroptosis :

Cell death characterised by excessive inflammation (caspase dependent) induced by the activation of inflammasome sensors like Nod-like receptor (NLR) family, the DNA receptor Absent in Melanoma 2 (AIM2) and the Pyrin receptor is called pyroptosis (68). DOX-induced pyroptosis is triggered by the increased expression of the NLR family pyrin domain-containing 3 (NLRP3) inflammasome. Once activated, NLRP3 facilitates the recruitment and activation of caspase-1. Active caspase-1 then promotes the activation of interleukins IL-1β and IL-18 while cleaving gasdermin D (GSDMD) into its N-terminal and C-terminal fragments. The N-terminal fragment of GSDMD binds to the plasma membrane, forming pores that result in cell swelling, membrane rupture, and the release of pro-inflammatory cytoplasmic components (69,70). The NLRP3/caspase-1/GSDMD pyroptosis pathway plays a significant role in inflammation. Additionally, DOX can promote the activation of the Bnip3-caspase-3-GSDME pathway which can induce cardiomyocyte pyroptosis (71). Inhibition of the NLRP3-caspase-1 or Bnip3-caspase-3-GSDME pathway using pharmaceutical interventions has proven to attenuate cardiomyopathy induced by DOX (71–73). Patient's undergoing DOX treatment exhibit elevated level of pro-inflammatory cytokines such as TNFα, which is known to exacerbate DOX linked cardiac dysfunction and toxicity (9,74). Understanding the inflammatory pathways for DOX's cardiotoxic effect and finding a therapeutic strategy to tackle it has gained interest of many researchers. A key inflammatory pathway is the cGAS-STING pathway.

**5. cGAS-STING inflammation pathway :**

The ability of the cell's innate immune system to detect microbial or viral infections is crucial for generating a defence response to eliminate the pathogen successfully (12). Cyclic GMP–AMP (cGAS) is a DNA sensor that recognises foreign genetic material or pathogen-associated molecular patterns (PAMPs) in the cytosol of the cell (75). The activation of cGAS by binding with DNA induces a conformational change to catalyses the synthesis of the secondary messenger cyclic guanosine monophosphate-adenosine monophosphate (cyclic GMP–AMP or cGAMP) from ATP and GTP (76). cGAMP binds and activate the transmembrane adaptor protein STING (stimulator of IFN genes/ TMEM173) which mainly resides in the endoplasmic reticulum (77,78). Activation of STING triggers the TANK binding kinase 1 (TBK1) and IFN-regulatory factor 3 (IRF3) signalling axis, resulting in the production and release of pro-inflammatory cytokines, such as type I interferons (IFNs) from the nucleus (77). The innate cGAS-STING pathway is essential for invoking an immune reaction against pathogenic stress. Ideally, the DNA material of a cell is contained in the nucleus and mitochondria. The DNA present in the cytoplasm is rapidly broken down by nucleases such as TREX-1 and DNase II. However, in a state of cellular stress and genomic instability, the endogenous DNA can be released into the cytoplasm and accumulate there, eliciting a sterile inflammatory response (79). Mitochondrial DNA is more susceptible to oxidative stress which can compromise its integrity and result in the release of mtDNA into the cytoplasm (80). Presence of cytosolic DNA act as a damage-associated molecular patterns (DAMPs) which are recognised through pattern recognition receptors (PRRs) (81). Hence, aggregation of cytosolic self-DNA along with reduced nuclease activity can activate the cGAS-STING signaling pathway, leading to an autoimmune inflammatory response (12). Cardiovascular diseases (CVDs) such as atherosclerosis, cardiac hypertrophy, DOX-induced cardiotoxicity and heart failure have been associated to genomic instability and excessive inflammation (82,83). Understanding the role

of cGAS-STING pathway can offer new insights into disease mechanisms and potential therapeutic strategies.

## 5.1 DAMPS

Sterile inflammation is a result of non-pathogenic stress (84). Pattern recognition receptors (PRRs) like Toll-like receptors (TLRs), NOD-like receptors (NLRs), and multiple intracellular DNA sensors are responsible for recognising endogenous molecules called damage-associated molecular patterns (DAMPs), which are released during cellular and tissue damage (85). High-mobility group box 1 protein (HMGB1) is a type of DAMP that activates TLR4 signalling in ischemia reperfusion injury (IRI), driving inflammation (86). Previous work from our laboratory has shown that as a result of DOX treatment there is loss of HMGB1 from the nucleus (7). Efflux of mtDNA and genomic DNA into the cytoplasm can serve as a DAMP which can be picked up by cytoplasmic DNA sensors cGAS and trigger an autoinflammatory reaction (85).

## 5.2 Activation of cGAS and production of cGAMP :

cGAS amino acid constituting of two domains – first highly basic ~160-amino-acid amino-terminal (N-terminal) unstructured domain and second globular ~360-amino-acid nucleotidyltransferase (NTase) (C-terminal) (75,81). cGAS which is unbound to DNA is not structurally active as its monomeric when free (87). The binding of double stranded DNA (dsDNA) induces confrontational change to form 2:2 oligomeric complex, where two cGAS molecules are associated with two dsDNA strands (88). This causes the catalytic pocket on the N-terminal to get activated and catalyzes the production of 2′3′-cGAMP from ATP and GTP (76). cGAMP has high affinity for STING and it acts as a secondary messenger which then activates STING (89).

5.3 Activation of STING and downstream effects :

STING resides in the transmembrane region of the endoplasmic reticulum (ER), where it exists as an inactive dimer. In this state, STING forms a V-shaped ligand-binding pocket designed to accommodate cyclic GMP-AMP (cGAMP) (90). Upon binding with cGAMP, the dimer undergoes structural stabilization, enabling its translocation from the ER to the Golgi apparatus (91). This translocation facilitates the recruitment of TANK-binding kinase 1 (TBK1) and interferon regulatory factor 3 (IRF3) to the C-terminal tail (CTT) of STING (79). TBK1 phosphorylates IRF3, activating this transcription factor, which subsequently enters into the nucleus (92). In the nucleus, IRF3 induces the expression of interferons and inflammatory cytokines, including TNF, IL-1β, and IL-6, resulting in a pro-inflammatory immune response (57). Stimulation of the cGAS-STING pathway release of nucleotide-binding oligomerization domain-like receptor pyrin domain containing 3 (NLRP3) inflammasome (93).

Though induction of inflammation is a crucial component for immune response and tissue repair (94). A tight regulation over pro-inflammatory and anti-inflammatory factors is necessary to maintain immune homeostasis. Excessive and prolonged inflammation can be detrimental as it can lead to autoimmune disorders.

5.4 Role of cGAS-STING in diseases :

cGAS-STING pathway is an important mediator for innate inflammation. There is evidence proving the involvement of the signalling pathway as a inducer of acute to chronic inflammation in various diseases pathologies (95). For instance, mutation in the endonuclease TREX1 causes Aicardi-Goutières syndrome that affects the functionality of the enzyme and has been shown to be involved in the pathogenies of Systemic lupus erythematosus (SLE) which is an autoimmune disease (96). Inability of TREX to degrade cytosolic dsDNA activates

cGAS-STING pathway leading to the development of the pathology seen in SLE (97,98). Grieves et al. demonstrated that restoring TREX1 function as a potential strategy to help mediate activation of unnecessary inflammation (99). Furthermore, research done by Li et al. indicates that inhibition of cGAS recuses the autoimmune inflammation response in Trex1$^{-/-}$ mice (100). Rheumatoid arthritis (RA) is associated with elevation in inflammatory responses through the cGAS/STING signalling pathway as a result of accumulation of cytosolic DNA. Overexpression of DNase II a lysosomal enzyme that digests DNA or knockdown of cGAS/STING reduces dsDNA-induced phosphorylation of IRF3 and NF-κB p65, mitigating the inflammatory signaling (101). Similarly, in DNaseII$^{-/-}$ mice exhibiting severe autoimmune and inflammatory phenotypes, inhibition of cGAS effectively averted these manifestations (102). Tumor metastasis is linked with chromosomal instability and cytosolic DNA sensing pathway activation. STING deficiency slowed down metastasis of tumor cells and decreased inflammatory pathway activation (103). STING induced IFN (type-I interferon) signalling drives elevation in pro-inflammatory cytokines in the case of traumatic brain injury (TBI), whereas STING$^{-/-}$ mice exhibited neuroprotection following TBI (104).

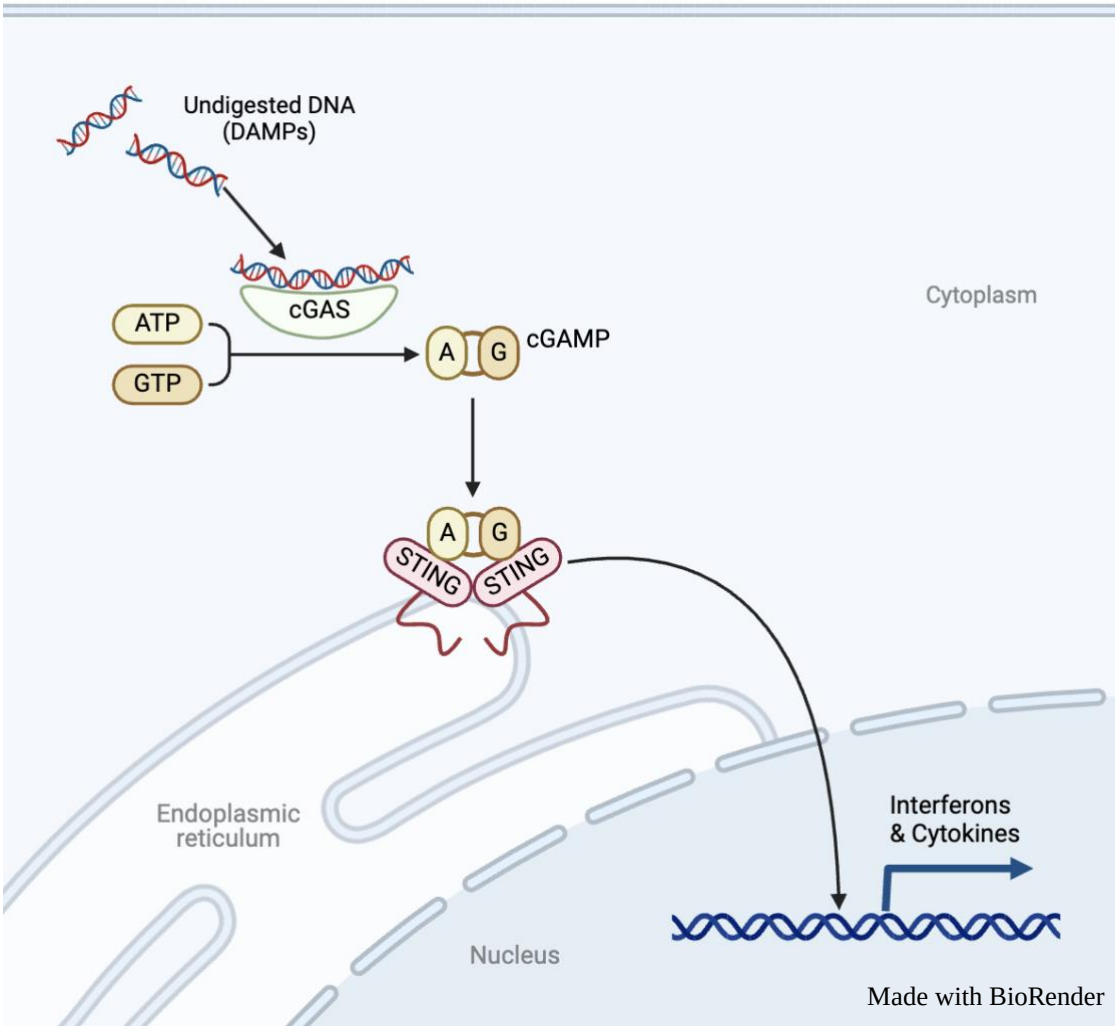


**Figure A. Schematic representation of cGAS-STING signalling pathway.**

Cellular stress leads to the release of DNA into the cytoplasm, which acts as a DAMP. This DNA is detected by the cytosolic DNA sensor cGAS. Upon binding to DNA, cGAS is activated and catalyzes the production of cGAMP. cGAMP functions as a second messenger, binding to and activating the STING protein located on the ER. STING activation triggers a signaling cascade that culminates in the production and release of type I interferons and pro-inflammatory cytokines, initiating an inflammatory response.

5.4.1 CVDs and cGAS-STING :

Recent studies suggest the activation of cGAS-STING signalling pathway due to high content of cytosolic self-DNA (mtDNA or nuclear) is an integral part of various cardiovascular diseases (CVDs) (105–107). Myocardial infarction causes extensive cardiomyocyte necrosis, resulting in the release of DAMPs triggering activation of innate immune pathways and initiate a robust inflammatory response (108). Although inflammatory response is necessary for clearance of death cells and to promote scar formation, prolonged inflammation can exacerbate cardiac injury (109). Large scale cardiac myocyte death as observed in MI, elicits a strong type I IFN signaling response from heart macrophages which is mediated by the cGAS–STING pathway (110–112). STING specific inhibitor H-151 treatment decreases inflammatory cells infiltration post MI and alleviates cardiomyocyte cell death and fibrosis of cardiac fibroblasts (113).

In angiotensin II (Ang II)-induced aortic aneurysm and dissection (AAD) upregulation of neutrophil cytoplasmic factor 1 (Ncf1) is crucial for preventing STING activation and chronic inflammation which leads to smooth muscle cell (SMC) apoptosis. Inhibition of STING is protective against aortic degeneration and AAD formation (114). Gene deletion of Trex1 in mice had extremely low survival rate and developed myocarditis causing cardiomyopathy and heart failure (115).

MI, heart failure, stroke and claudication are different types of CVDs that can be caused as a result of atherosclerosis (108). Release of endogenous DNA fragments is part of atherosclerosis pathogenesis which can trigger inflammation through STING activation (116). Hence, inhibition of STING either pharmaceutically or genetically can be a potentially strategy to mediate inflammation and plaque formation in atherosclerosis (116,117).

Studies have shown correlation between CVDs, elevated levels of inflammatory markers and cGAS-STING pathway activation. Inflammatory reaction plays a significant role in progression of cardiovascular diseases. A chronic inflammatory response can lead to impaired

left ventricular function, development of cardiac fibrosis, adverse cardiac remodeling, and ultimately, cardiomyocyte death. These pathological changes collectively exacerbate the severity and progression of CVDs, highlighting the critical role of inflammation and cGAS-STING signaling in cardiovascular pathophysiology (83).

DOX-induced cardiomyopathy is a serious risk factor for the clinical use of the chemotherapy drug (3). Inflammation is known to be involved in the pathogenesis of the anthracycline-induced cardiotoxicity (118). DOX treatment elicits production of proinflammatory cytokines like interleukin (IL)-1β, IL-18, IL-6 and TNF-α (9,74,119). This inflammatory response further amplifies the cardiac injury induced by DOX.

Accumulating literature suggest that targeting and suppressing inflammatory pathway could serve as a promising therapeutic strategy to mitigate the damage caused by excessive inflammation in various disease states (120).

However, the exact mechanism for cGAS-STING inflammatory pathway's link to DOX induced cardiotoxicity remains elusive and needs more research. In this study, we explore the role of the cGAS-STING pathway in doxorubicin-induced cardiomyopathy to identify potential therapeutic strategies.

## Rationale and Hypothesis

### Rationale :

Clinical observations have shown that cancer patients undergoing DOX chemotherapy have elevated levels of inflammation as a manifestation of DOX-induced toxicity. Recent studies indicate that cardiovascular disorders such as myocardial infarction and aortic aneurysm and dissection is closely linked to increased inflammatory response and activation of cGAS – STING innate immune pathway. Whether DOX-induced inflammatory reaction is connected to the activation of the cGAS-STING pathway remains elusive and requires further research. Hence in this study we investigate the role of cGAS-STING signalling in DOX-induced cardiomyopathy.

### Hypothesis :

Impaired autophagy activates the innate cGAS-STING signaling pathway resulting in pro-inflammatory responses and cardiac dysfunction in DOX cardiomyopathy.

## Materials and Mythologies

### 1. Neonatal rat cardiomyocyte (NCMC) isolation and cell culture :

Neonatal rat ventricular myocytes were isolated from the excised hearts of 1-2 days old Sprague-Dawley rat pups. The extracted hearts underwent enzymatic digestion followed by Percoll gradient centrifugation to obtain a primary cardiomyocyte culture. Cells were incubated to overnight in Dulbecco's modified Eagle's medium (DMEM)/F-12 (DF) nutrient mixture in a ratio of 1:1 at 37°C. The nutrient media DMEM/F-12 is supplemented with 17 mmol/L HEPES, 3 mmol/L NaHCO3, 2 mmol/L l-glutamine, 50 µg/mL gentamicin, and 10% FBS. The following day the cell culture media was replaced with DF serum free (DFSF) media. Cells were plated for 24 hours before being subjected to respective treatment.

To study the dose dependant effect of DOX treatment, myocytes were treated with increasing doses of DOX (0.5µM, 1µM, 2.5µM, 5µM and 10µM, Pfizer Canada) for 18hr.

Additionally, NCMC were treated with DOX (0.5µM) along with cGAS inhibitor (RU.521) in different dose concentration (0.5µM, 1µM, 2.5µM and 5µM) for 18hr before testing for different end points. Similarly, STING inhibitor (H151) was used as an intervention in various concentration for DOX (0.5µM) treatment.

### 2. Western blot :

At the end of the treatment, cardiac myocytes were lysed using Radioimmunoprecipitation assay buffer (RIPA) (1.0% deoxycholate, 140 mM NaCl, 10 mM Tris-HCl, 1% Triton X-100 and 0.1% SDS) with protease inhibitors (10µl of NaF, 10µl of PI, 10µl of Na3VO4, and 3.4µl PMSF per 1mL of RIPA). Bicinchoninic acid (BCA) assay (Thermo Fisher Scientific, 23225) was done to determine the protein concentration in each sample. For western blot analysis, cardiomyocyte lysates (20 µg protein per sample) were denatured at 100°C for 5 mins. Protein

extracts were resolved in a denaturing sodium dodecyl sulfate–polyacrylamide gel electrophoresis (SDS-PAGE) gels and then transferred onto a nitrocellulose membranes (Bio-Rad, 1620094). The membranes were probed overnight at 4°C with primary antibodies targeting DNase II, TREX1, cGAS, STING, NLRP3, Bnip3, GAPDH, $\beta$-Tubulin and $\alpha$-Actin. The primary antibodies were made using a 1:1000 dilution with 2.5% skimmed milk in TBS-T (50mM Tris-HCl, 150mM NaCl, 0.3% Tween- 20, pH 7.4). The following day, the membrane were washed with TBST for 10 mins each and then incubated with a secondary antibody-horseradish peroxidase (HRP) conjugate (anti-murine or anti-rabbit respectively) for 1 hour at room temperature. Chemiluminescence was used to detect desired protein bands on the western blot.

**3. Cell viability assay :**

Myocytes were plated at a density of $3.2x10^5$ cells per well on glass coverslips for staining. At the end of treatment, the cells were incubated with florescent dyes to asses cell viability. 2 μM of calcein acetoxymethyl ester (Calcein-AM, InvitrogenTM C3100MP) was used to stain live cells green and 2 μM of ethidium homodimer-1 to label dead cells red. The working solution for cell viability staining was prepared by adding 8μl of Calcein and 2μl of ethidium homodimer-1 to 10ml DFSF media. The cells were incubated for 30 minutes in 37°C in the working solution after treatment. After incubation, the cells were visualized using Olympus AX-70 research fluorescence microscope at x200 magnification. The images were captured using Zeiss ZEN 3.3 software and analysis was performed on ImageJ software. For each condition at least ≥200 cells were counted from three independent repeat experiments.

**4. Mitochondrial permeability transition pore opening assay :**

Mitochondrial permeability transition pore (mPTP) opening of cardiomyocytes cultured on coverslips was evaluated by florescent staining with 5 μmol/L calcein-AM (Molecular Probes) and 2 mmol/L cobalt chloride. In 10ml DFSF media, 8μl of calcein and 50μl of cobalt chloride was add to make the working solution. Cells were incubated in the media for 30 minutes in 37°C post intervention. Coverslips were inverted onto a glass slide and changes in the florescence intensity of the cells were visualised using Olympus AX-70 research fluorescence microscope at x600 magnification. Decrease in intensity of the calcein-AM (green) florescence indicated opening of mPTP. Individual cell florescence was measured using ImageJ software.

**5. Reactive oxygen species production assay :**

To analyse the amount of reactive oxygen species (ROS) produced in each condition cells were fluorescently stained with 2.5μM of Dihydroethidium (Molecular Probes) dissolved in DFSF (1μl of Dihydroethidium per 1ml DFSF media). Cells were incubated for 30 minutes in 37°C temperature. Coverslips for each condition was placed on a glass slide for observation using Olympus AX-70 research fluorescence microscope at x200 magnification. ROS production was signified by higher intensity of the red florescent staining. ImageJ software was used to analyse the intensity of the whole image captured using Zeiss ZEN 3.3 software.

**6. Mitochondrial Membrane Potential (ΔΨm) :**

Florescent reagent tetra-methylrhodamine methylester perchlorate, 50nM (TMRM, Molecular Probes) was used to determine mitochondrial membrane potential (ΔΨm) in cells. Cells were treated with TMRM fluorogenic dye for 30 minutes in 37°C incubator. Via epifluorescence microscopy the cells were visualised and captured on Olympus AX-70 research fluorescence

microscope at x600 magnification using Zeiss ZEN 3.3 software. Lower intensity of the red TMRM dye signified loss in ΔΨm. The analysis was performed using ImageJ software by measuring the intensity of florescence of each cell.

**7. Co-localization between GFP-LC3 and NucBlue :**

GFP-LC3 (green fluorescent protein – LC3) adeno-virus was used to tag autophagosomes green. NucBlue (Hoechst 33342), a nuclear counterstain, was used to visualise the presence of DNA in live cardiomyocytes and nuclear morphology as the dye emits blue florescence when bound to DNA. Carl Zeiss spinning disc confocal microscope was used to capture live images of the cells in 2D and 3D, at 630x or 1000x magnification with ZEN software. Co-localization between GFP-LC3 puncta and NucBlue staining was analysed with Pearson's coefficient with ZEN software in the area of interest. Higher value of Pearson's coefficient indicated greater co-localization between the two staining. Z-stack 3D imaging using Zeiss confocal fluorescence microscope reflected the level of co-localization measured between GFP-LC3 and NucBlue staining.

**8. Human Patients Sample Collection (Left Ventricular Tissue) :**

Human left ventricular (LV) tissue sample obtained for a prior study conducted in our lab and previously described (9) were used for western blot analysis.

**9. Statistical analysis :**

Quantitative data are presented as the mean ± standard error of the mean (SEM). For comparisons between two groups, an unpaired two-tailed Student's t-test was applied. Comparisons between multiple groups were performed using one-way analysis of variance

(ANOVA), followed by Tukey's post hoc test. Statistical significance was measured with Graph Pad Prism 6 and 9 software. In all cases, the data was derived from minimum of three independent repeat experiments, with differences considered statistically significant at *P < 0.05, **P < 0.01, or ***P < 0.001.

## Results

### 1. cGAS-STING inflammatory pathway is activated in cancer patients and in rat ventricular myocytes post Doxorubicin (DOX) treatment :

Previous studies, including work from our lab, have established the role of inflammatory cytokines like TNF- α in the pathogenesis of DOX-induced cardiomyopathy (9,74). Building on that foundation, we investigated whether cGAS-STING pathway is activated in cancer patients who had suffered from heart failure following DOX chemotherapy. Western blot analysis was performed on human heart tissue samples. The result as illustrated in Figure 1.1, revealed that the expression of the STING protein is significantly upregulated in the cardiac tissue of cancer patients who had received DOX chemotherapy, in contrast to the expression levels observed in normal human hearts samples.

To validate our initial findings, we conducted experiments on neonatal cardiomyocytes (NCMCs). The NCMCs were exposed to DOX treatment for 18 hours. The cells were treated with 0.5μM, 1μM, 2.5μM, and 5μM concentration of DOX. The western blot analysis depicted in Figure 1.2 showed dose dependent elevation in expression of cGAS and STING proteins compared to untreated control cells. These observations confirm that activation of the cGAS – STING inflammatory pathway in cardiac myocytes in response to DOX.

Furthermore, the western blot analysis in Figure 1.2 also demonstrated an increase in the protein expression of NLRP3, an inflammasome component, particularly at higher concentration of DOX treatment (5 μM).

These results indicate that an inflammatory response is triggered in cardiac myocytes when subjected to DOX treatment via the activation of cGAS – STING signalling pathway.

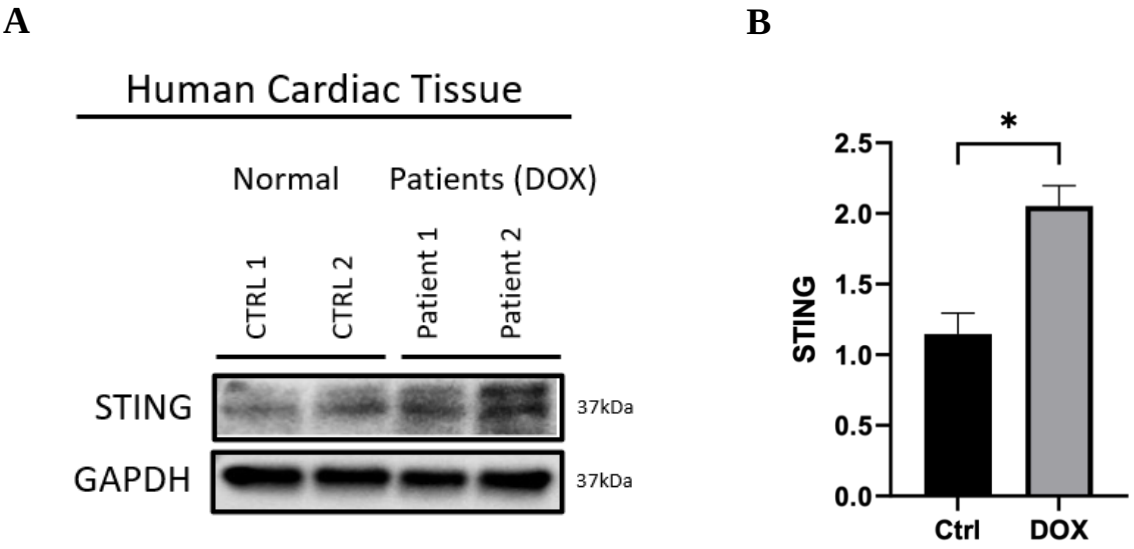


**Figure 1.1 Increased expression of STING protein in the hearts of cancer patients receiving Doxorubicin (DOX) chemotherapy treatment**

**Panel A.** Western Blot (WB) analysis of human left ventricular (LV) tissue lysate derived from patients treated with DOX (lanes 3 and 4) and from normal hearts that were donated for transplantation (CTRL; lanes 1 and 2).

**Panel B**. Quantitative analysis of STING protein expression of Panel A illustrated as a bar graph. Statistical significance marked by *P<0.05.

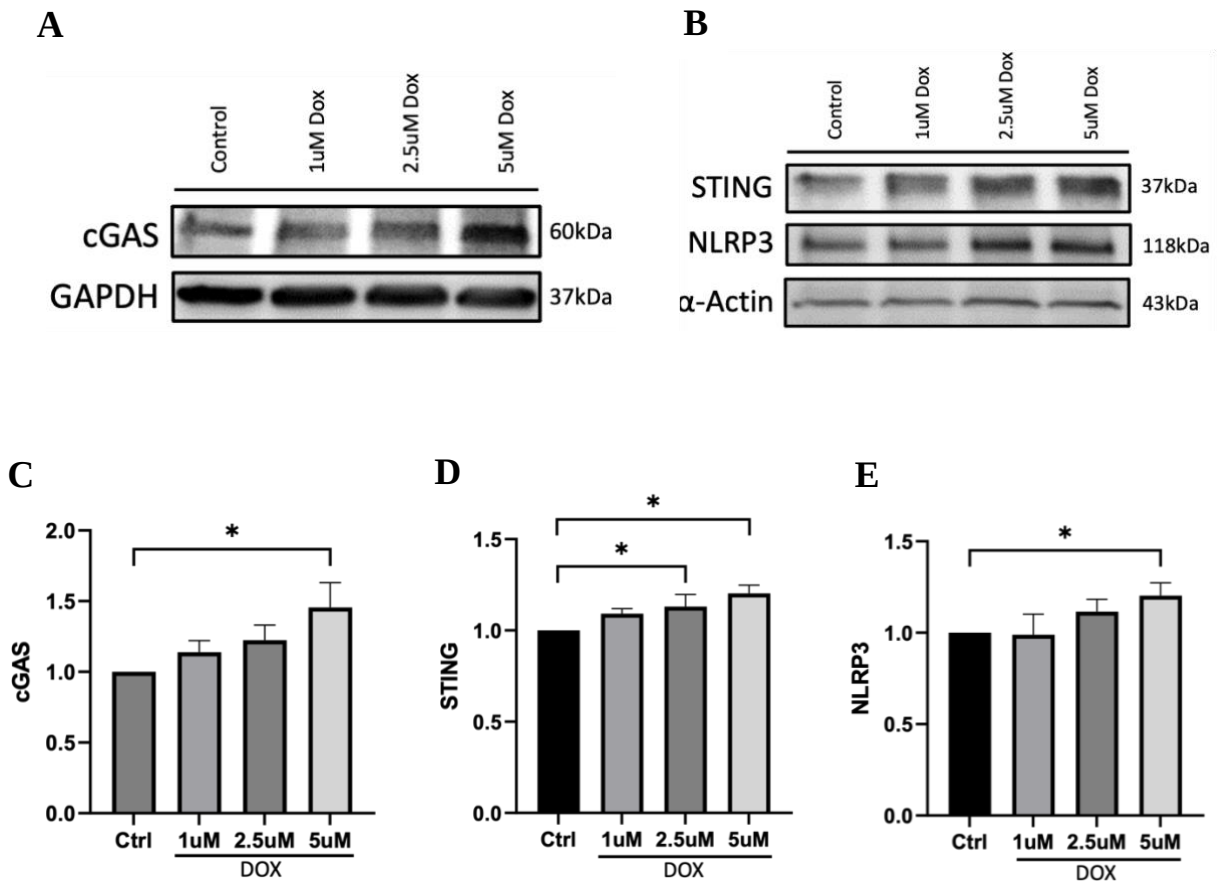


**Figure 1.2 DOX activates the cGAS-STING inflammatory pathway in rat ventricular myocytes**

**Panel A-B.** Western blot analysis showing dose-dependent upregulation of cGAS, STING, and NLRP3 protein expression in rat ventricular myocytes treated with increasing concentrations of DOX (1–5 μM).

**Panel C-E.** Quantitative analysis of protein expression levels for cGAS, STING, and NLRP3, respectively, normalized to control. Data are presented as mean ± SEM. Statistical significance is indicated by *P < 0.05 compared to untreated control.

**2. DOX treatment induces cytoplasmic DNA accumulation, DNase II depletion and HMGB-1 mediated cell death in cardiac myocytes :**

To understand the molecular mechanism underlying the activation of cGAS - STING inflammation pathway in response to DOX, it was vital to investigate and identify potential triggers. NCMCs cultured on chamber slides were infected with an adenovirus encoding the autophagy reporter GFP-LC3 (green florescent protein – LC3). The following day the cells were treated with DOX (5μM) for 18 hours. Subsequently, the cells were visualised using confocal microscopy with the live NucBlue staining to tag DNA and nuclear morphology in the cell.

Figure 2.1 shows the contrasting effect of DOX treatment on NCMCs compared to control condition. In untreated cells it was observed that the nuclear NucBlue dye (blue color) stays confined in the nucleus, while the GFP-LC3 puncta (green color) representing autophagosomes are visible throughout the cytoplasm. However, DOX treated cardiac myocytes exhibit a striking difference. It was found that the NucBlue staining leaks into the cytoplasm. This indicates the presence of DNA material outside of the nucleus.

The presence of cytoplasmic DNA serves as DAMPs which can then be detected by cGAS DNA sensor molecule hence triggering the activation of the cGAS-STING signalling pathway. The 3D imaging illustrated in Figure 2.1 A, shows that GFP-LC3 puncta is engulfing the blue DNA staining suggesting the initiation of the autophagy process. This was then analysed using the Pearson's coefficient analysis on ZEN software to determine the co-localization between the GFP-LC3 puncta and DNA blue staining in the area of interest. The analysis proved that the co-localization between the two is significant in the DOX condition.

Based on previous research that has demonstrated that DOX impairs the autophagy process (11), our findings suggest that autophagy is initiated but not effectively completed. The impairment of autophagy could lead to accumulation of undigested autophagosome.

Consequently, accumulation of cytoplasmic DNA is observed under DOX treatment which can present as DAMPs.

Another key factor for activation of the cGAS-STING pathway is the absence or reduction in the presence of exo or endonucleases. DNase II protein is an acidic endonuclease and is responsible for degradation of DNA within the lysosome (121). Western blot analysis shown in Figure 2.2 exhibits that the expression of DNase II gets significantly reduced when treated with DOX in a dose dependent manner. Without the presence of nuclease, the DNA would remain in the cytoplasm undegraded.

HMGB-1 is a well-known DAMP which can provoke cell death by activation of STING (122). A previous work from our lab shown that there is loss of nuclear HMGB-1 as a response to DOX treatment (7). Based on that, our aim was to investigate whether HMGB1 inhibition could mitigate DOX-induced toxicity. Cardiac myocytes were treated with DOX (5μM) along with HMGB-1 inhibitor (HMGB-1-IN). It was found that cell death induced by DOX treatment was suppressed by the inhibition of HMGB-1. The cell death induced by DOX is significantly reduced using the inhibitor in increasing doses ranging from 0.5 to 10μM, as shown in Figure 2.3.

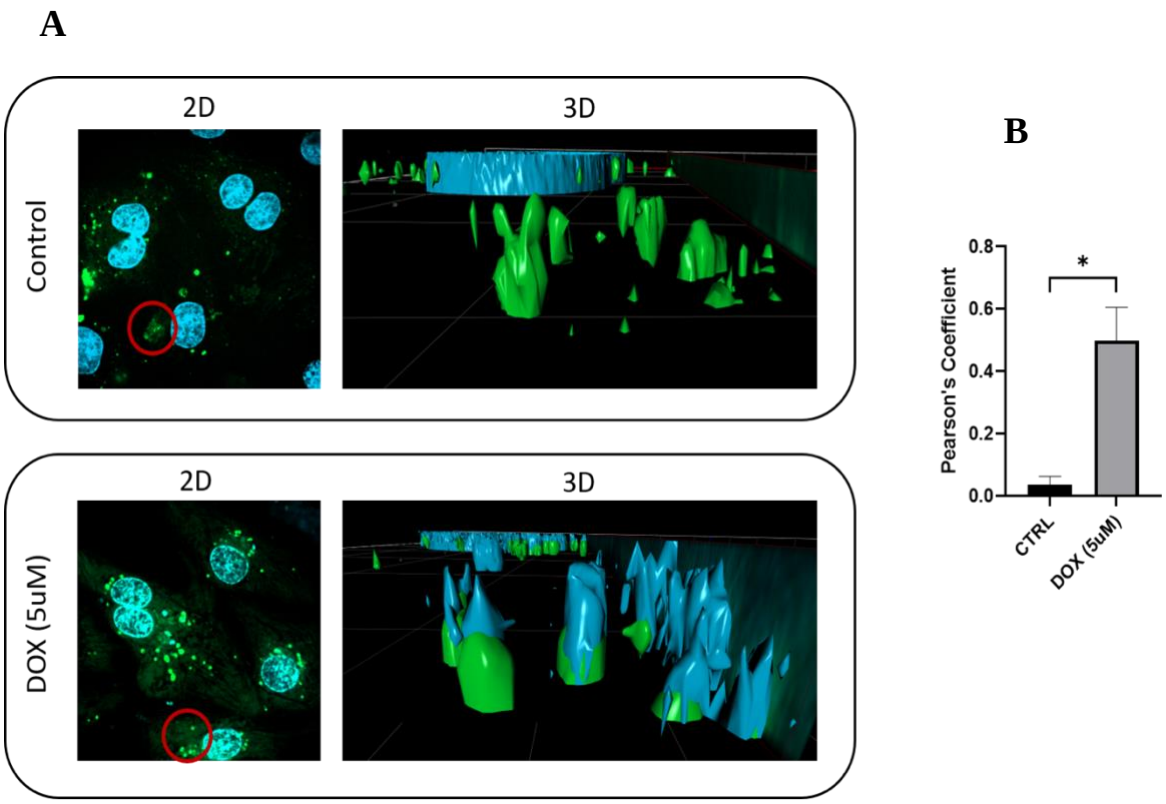


**Figure 2.1 Presence of cytoplasmic DNA**

**Panel A.** Representative confocal image of saline- (Control) and doxorubicin (DOX)-treated cardiac myocytes. GFP-LC3 stained autophagosomes green and NucBlue stained DNA content blue. Images on the left show the normal 2-D view and on the right shows the 3-D and colocalization of the two staining in DOX condition.

**Panel B.** Colocalization between GFP-LC3 and NucBlue staining is illustrated by the histogram, showcasing the Pearson correlation coefficient as a measure of this relationship. The statistical significance of the difference between CTRL and DOX was determined using Student's T-Test, *P < 0.05.

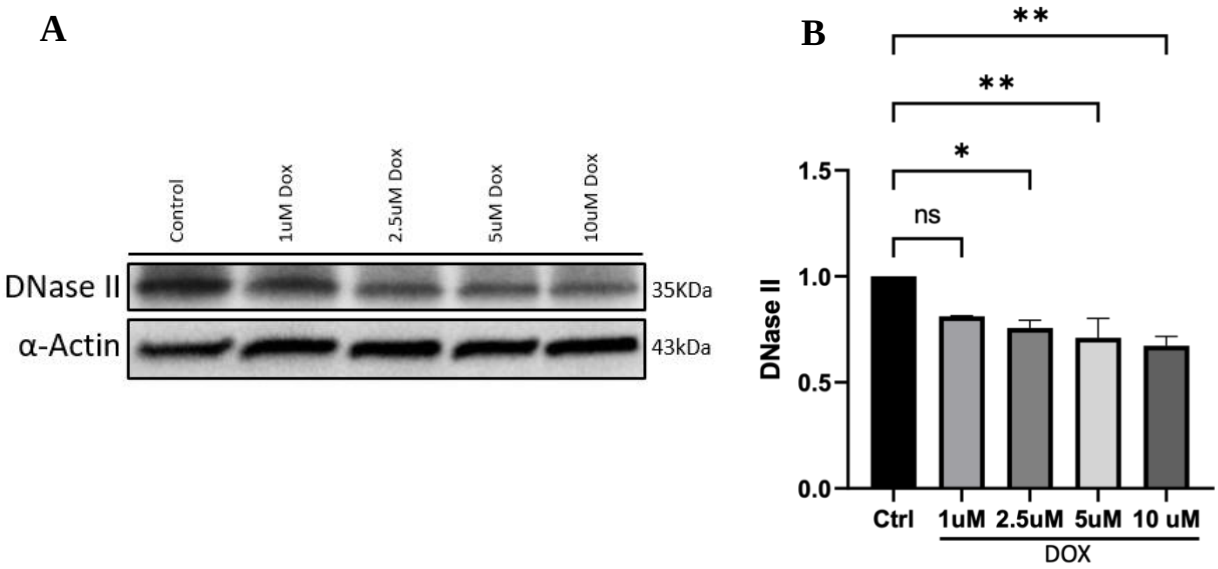


**Figure 2.2 Decrease in DNase II protein expression in cardiac myocytes with DOX treatment**

**Panel A.** Western blot analysis of cardiac myocyte lysate treated with increasing dose concentration of DOX. The western membrane was probed with primary antibody directed towards DNase II protein.

**Panel B.** Quantitative data for normalized DNase II protein shown in Panel A. The statistical significance from CTRL compared to other conditions are represented as *P < 0.05 and **P < 0.01

**A**

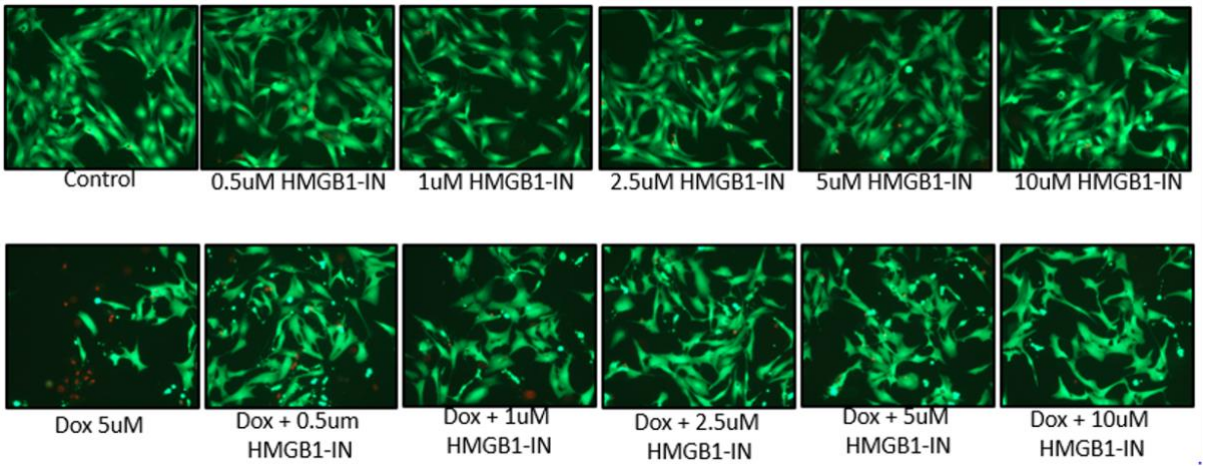


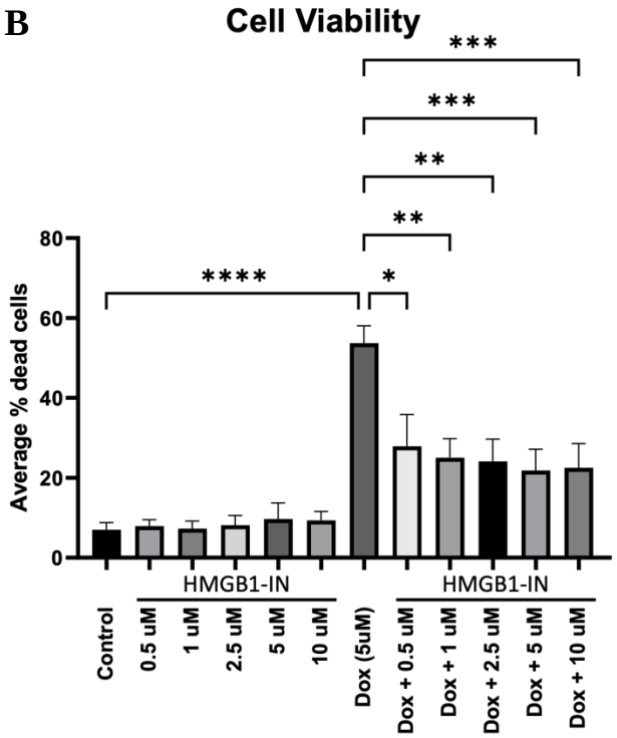


**Figure 2.3 Inhibition of HMGB1 DAMP reduces cell death induced by DOX**

**Panel A.** Epifluorescence microscopy for cell viability assay of neonatal ventricular myocytes in control (CTRL) and DOX treatment in the presence of HMGB1 inhibitor (HMGB1-IN) in increasing doses (0.5-10 μM). Live and death cells are stained green and red respectively.

**Panel B.** Histogram showing quantitative data for the conditions in Panel A. Statistically different from average percentage of death cells from DOX-only condition; *P < 0.05, **P < 0.01, or ***P < 0.001.

**3. Mitochondrial death protein (Bnip3) is induced by DOX :**

Bnip3 is a pro-apoptotic member of the Bcl2 family. Upon activation, Bnip3 integrates into the mitochondrial outer and inner membranes, where it exerts detrimental effects. Bnip3 causes mitochondrial perturbations and dysfunction resulting in cell death by disrupting the integrity of the mitochondria inner membrane resulting in impaired electron transport and complex IV activity (123). Previous work from our lab has shown that DOX induced cardiotoxicity is mediated by Bnip3 (7). We confirm this finding as we observed a dose dependent increase in Bnip3 protein expression and cell death following DOX treatment, shown in Figure 3.1.

Additionally, through cell viability assay it was found that, DOX induces wide spread cell death, evident by greater amount of red-stained dead cells in DOX-treated condition, Figure 3.2 A. To asses mitochondrial health, we conducted mitochondrial function assays after DOX treatment. Following Dox treatment, we observed a marked increase in ROS production, mitochondrial permeability transition pore opening and loss of mitochondrial membrane potential ($\Delta\Psi m$). Collectively, these findings show that DOX induced mitochondrial perturbations is mediated by a mechanism involving Bnip3 activation.

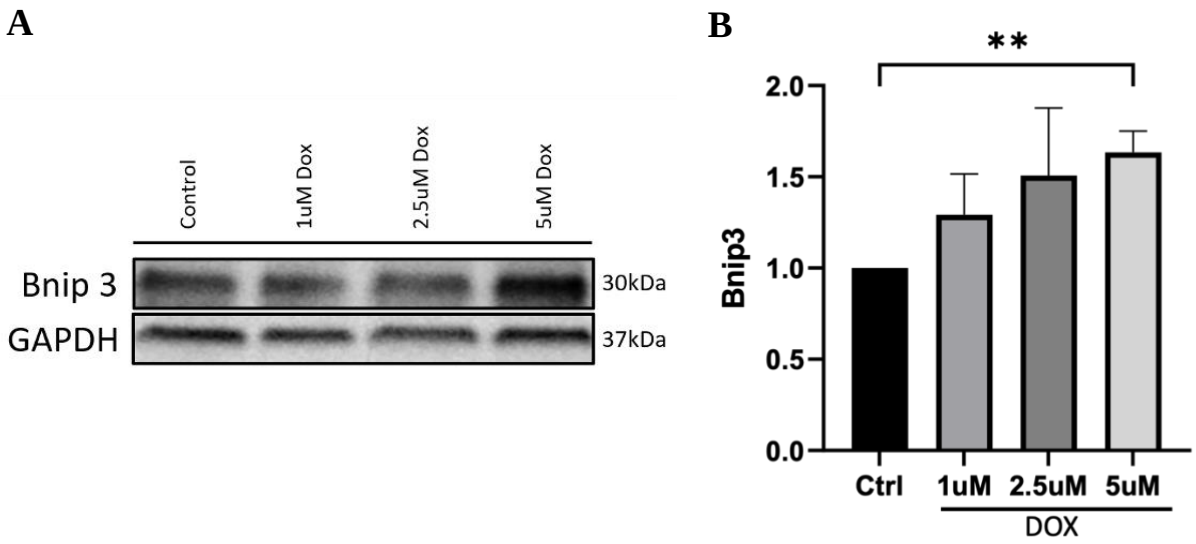


**Figure 3.1 Mitochondrial death protein (Bnip3) is induced by DOX**

**Panel A.** Western blot analysis showing dose-dependent increase in Bnip3 protein expression in ventricular myocytes treated with increasing concentrations of DOX.

**Panel B.** Quantitative analysis of Bnip3 protein expression normalized to control. Data are presented as mean ± SEM. Statistical significance is indicated by **P < 0.01 compared to untreated control.

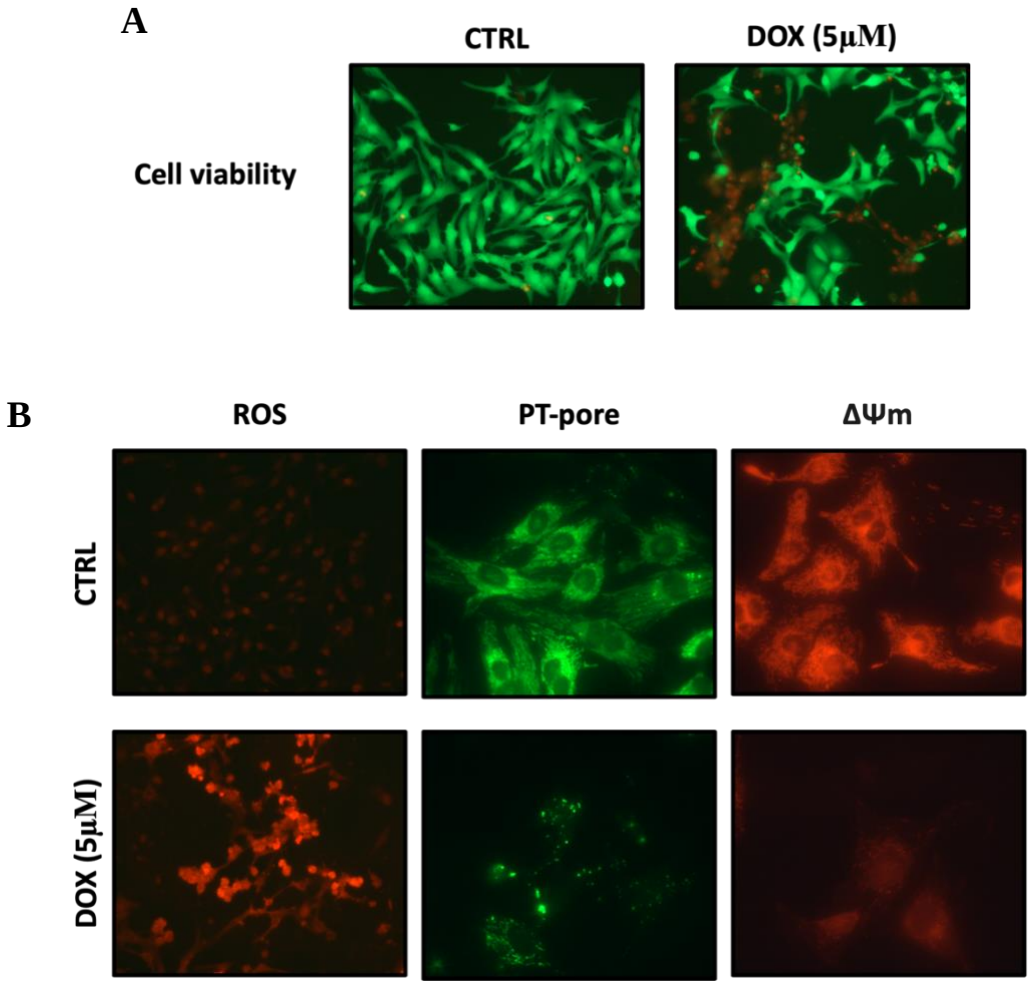


**Figure 3.2 DOX causes mitochondrial perturbations**

**Panel A.** Representative epifluorescence microscopy images of control (CTRL) and Doxorubicin (DOX) treated ventricular myocytes for cell viability assay. Cells were stained with vital dyes calcein-AM and ethidium-homodimer to detect the live (green) and dead (red) cells.

**Panel B.** Mitochondrial function assay for ROS (Left, red), mPTP opening (Center, green), and mitochondrial ΔΨm (Right, red) in control (CTRL) and Doxorubicin (DOX) treated cardiac myocytes.

**4. Inhibition of the innate cGAS-STING pathway reduces cell death induced by DOX :**

Given that the inflammatory cGAS – STING pathway is activated by DOX treatment, our next step was to examine whether blocking this pathway can have a cardioprotective effect. cGAS (RU.521) and STING (H151) inhibitors were used individually alongside DOX treatment to test the outcome of blocking the innate pathway.

Based on our previous findings, we treated the cells with a concentration of 5 μM of DOX. This dosage was chosen because it effectively elicited significant cellular responses, creating an optimal experimental condition for investigating DOX-induced cardiotoxicity, without promoting widespread cell death. NCMCs were treated with DOX in combination with either a cGAS or STING inhibitor. The cells received various concentrations of the inhibitor: 0.5 μM, 1 μM, 2.5 μM, and 5 μM. After 18 hours of treatment, the results from the cell viability assay indicated that DOX induced a significant level of cell death in NCMCs, with approximately a fourfold increase in cell death.

Interestingly, inhibition of the cGAS – STING pathway significantly suppressed the cell death caused by DOX. The most pronounced protective effect was seen at 1μM and 2.5μM dose concentration for both inhibitors, as shown in Figure 4.1 and 4.2 These findings suggest that blocking the cGAS-STING inflammatory pathway confers a protective effect against DOX-induced cardiotoxicity.

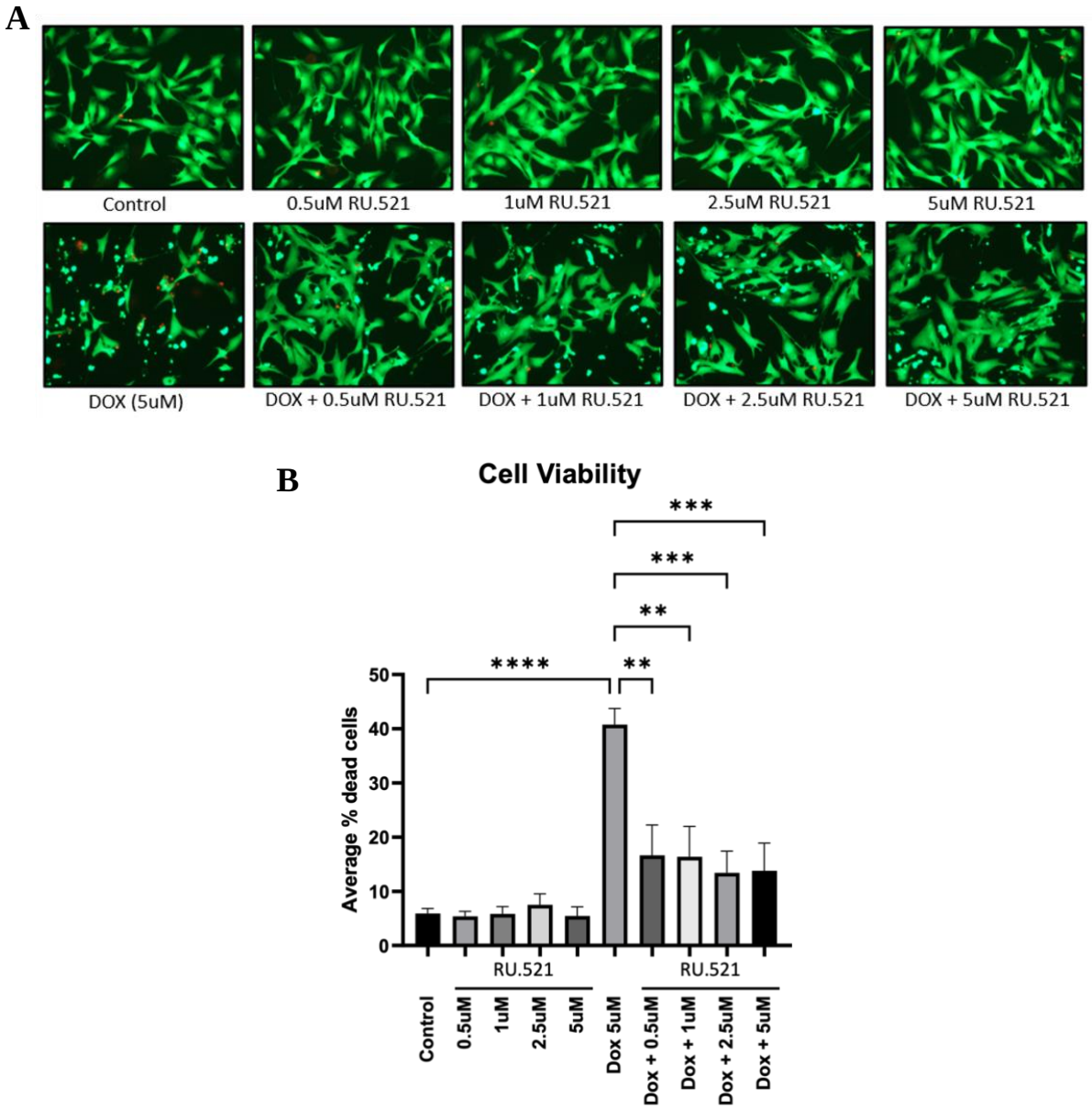


**Figure 4.1 Cell death induced by DOX is rescued using cGAS inhibitor, RU.521**

**Panel A.** Treating cardiac myocytes with cGAS inhibitor, RU.521 suppresses DOX-induced necrotic cell death. Epifluorescence microscopy for cell viability, living cells (green), dead cells (red) for ventricular myocytes in the absence and presence of DOX (5μM) along with RU.521 in increases concentration (0.5μM - 5μM).

**Panel B.** Histogram showing quantitative data for the conditions in Panel A. Statistically different from average percentage of death cells from DOX-only condition; *P < 0.05, **P < 0.01, or ***P < 0.001.

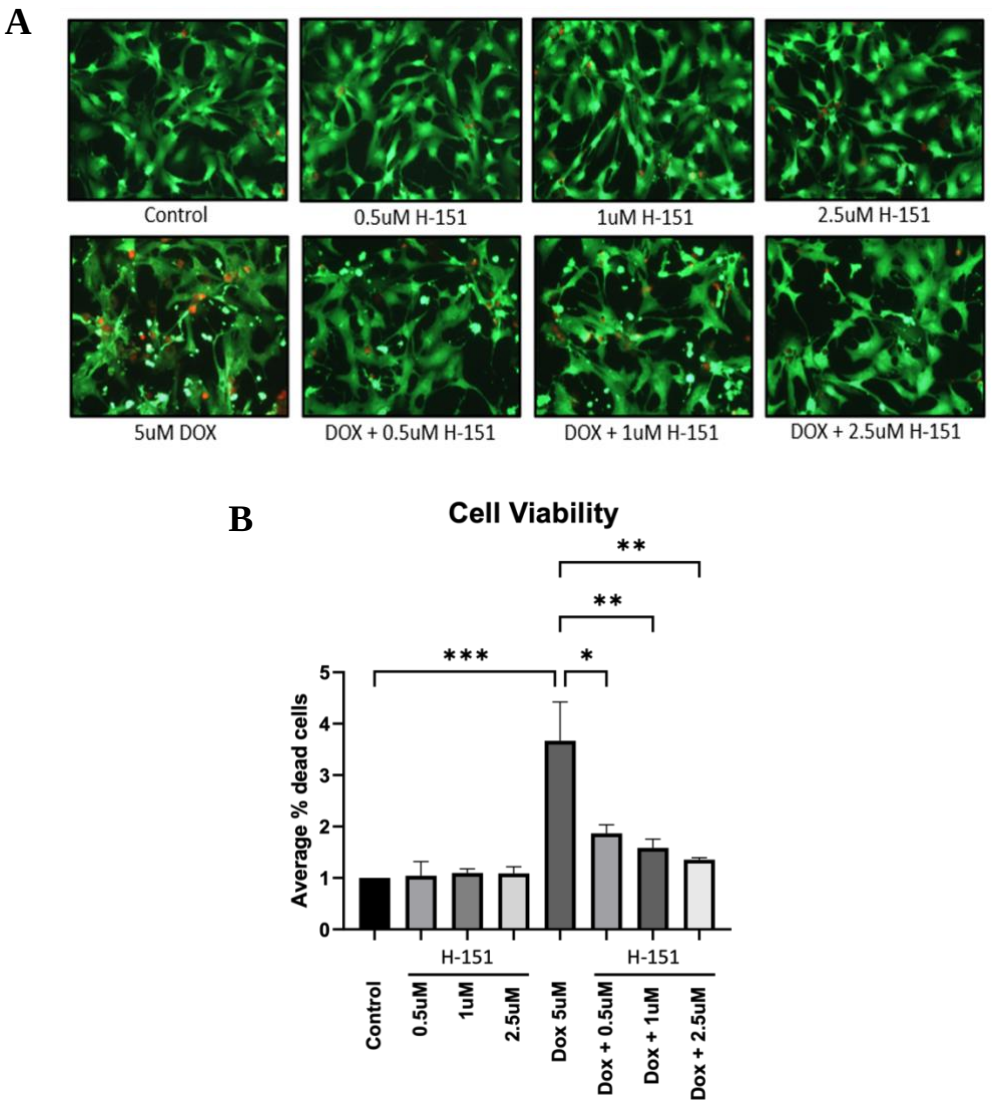


**Figure 4.1 Cell death induced by DOX is rescued using STING inhibitor, H-151**

**Panel A.** Representative epifluorescence images of cardiac myocytes subjected to cell viability assay. Cells were treated with or without doxorubicin (DOX, 5 μM) and varying concentrations of the STING inhibitor H-151 (0.5-2.55 μM). Live cells are visualized in green, while dead cells appear red.

**Panel B.** Quantitative analysis of cell death. The histogram depicts the average number of dead cells per field across different treatment conditions. Statistical significance is indicated as *P < 0.05, **P < 0.01, and ***P < 0.001 compared to the DOX-only condition.

**5. Mitochondrial perturbations induced by DOX was suppressed by inhibition of cGAS - STING pathway :**

In order to analyze the impact of blocking the cGAS – STING signalling pathway on cardiac myocytes treated with DOX, we proceeded to examine the mitochondrial health. DOX targets mitochondria, activating Bnip3 and inducing mitochondrial perturbations that lead to cell death (7,42). For the experiment, cGAS (RU.521) and STING (H151) inhibitors were applied at 1 μM and 2.5 μM concentrations, which exhibited the most cardioprotective effect by effectively suppressing cell death induced by DOX.

Reactive oxygen species (ROS) production assay was conducted with DOX (5μM) treatment, either alone or in combination with cGAS and STING inhibitors. In the DOX-only treatment condition, we observed an increased ROS production, represented by high intensity of the red-dihydroethidium staining, Figure 5.1. Strikingly, when the cells were treated with either cGAS or STING inhibitor alongside DOX, a significant reduction in ROS production in cardiac myocytes was noted.

Similarly, after 18 hours of treatment of cardiac myocytes for the conditions: control (CTRL), doxorubicin (DOX), DOX with cGAS inhibitor RU.521 (1 μM and 2.5 μM), and DOX with STING inhibitor H-151 (1 μM and 2.5 μM), mitochondrial function assays for mitochondrial permeability transition pore (mPTpore) opening and loss of mitochondrial membrane potential ($\Delta\Psi m$) was performed. Mitochondrial dysfunction caused by DOX in the form of mPTpore opening and loss of ($\Delta\Psi m$) was observed as reduction in the intensity respective staining in DOX-only condition, shown in Figure 5.2 and 5.3. Importantly, in the conditions where the cGAS and STING inhibitors were given the mitochondrial defects induced by DOX were mitigated.

In addition, cGAS (RU.521) and STING (H151) inhibitors not only reduced the expression of their target proteins but also diminished the expression of mitochondrial death protein Bnip3

and NLRP3 inflammasome, Figure 5.4 and 5.5. This comprehensive testing suggests that inhibition of the cGAS – STING signalling pathway effectively ameliorates DOX-induced mitochondrial perturbations induced by Bnip3 as well as attenuates inflammatory response, supporting the notion that Bnip3 mediated mitochondrial injury underlies inflammation and cell death of cardiac myocytes treated with DOX.

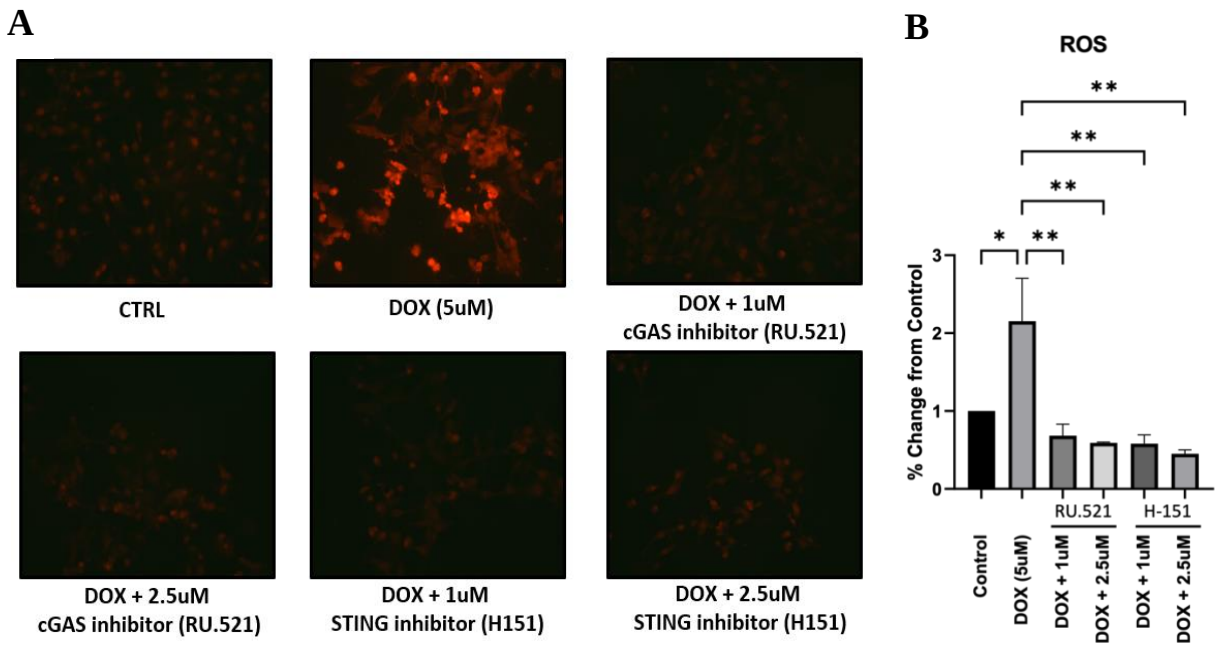


**Figure 5.1 Inhibition of cGAS and STING attenuates DOX-induced reactive oxygen species production in ventricular myocytes**

**Panel A.** Representative epifluorescence microscopy images of cardiac myocytes showing reactive oxygen species (ROS) production under various treatment conditions: control (CTRL), doxorubicin (DOX), DOX with cGAS inhibitor RU.521 (1 µM and 2.5 µM), and DOX with STING inhibitor H-151 (1 µM and 2.5 µM).

**Panel B.** Quantitative analysis of ROS production. The histogram represents mean fluorescence intensity for each treatment condition, normalized to control. Statistical significance is indicated by asterisks, where *P < 0.05, and **P < 0.01compared to the DOX-only condition.

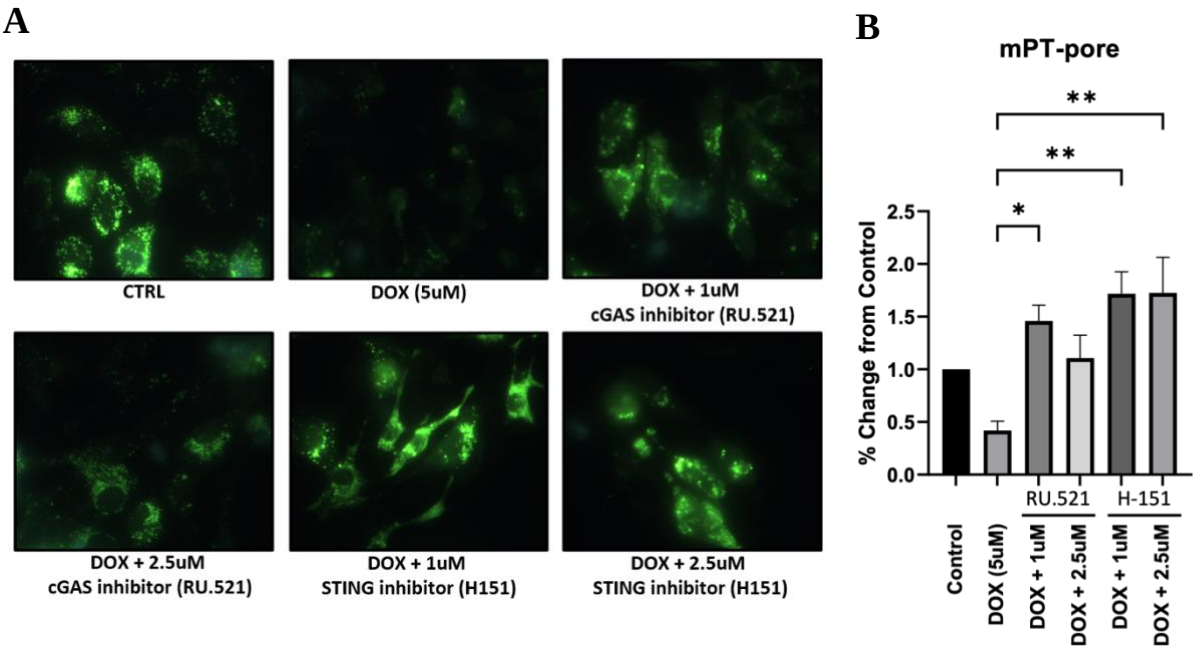


**Figure 5.2 cGAS - STING pathway inhibition mitigates DOX-induced mitochondrial permeability transition pore opening in ventricular myocytes**

**Panel A.** Representative epifluorescence microscopy images of ventricular myocytes stained with mitochondrial calcein-AM-CoCl2 (green) to assess mitochondrial permeability transition (mPT) pore opening. Diminished green fluorescence indicates mPT pore opening. Treatment conditions include: control (CTRL), doxorubicin (DOX), DOX with cGAS inhibitor RU.521 (1 µM and 2.5 µM), and DOX with STING inhibitor H-151 (1 µM and 2.5 µM).

**Panel B.** Quantitative analysis of mPT pore opening. The histogram displays mean fluorescence intensity for each treatment condition, normalized to control. Statistical significance is compared to the DOX-only condition: *P < 0.05 and **P < 0.01.

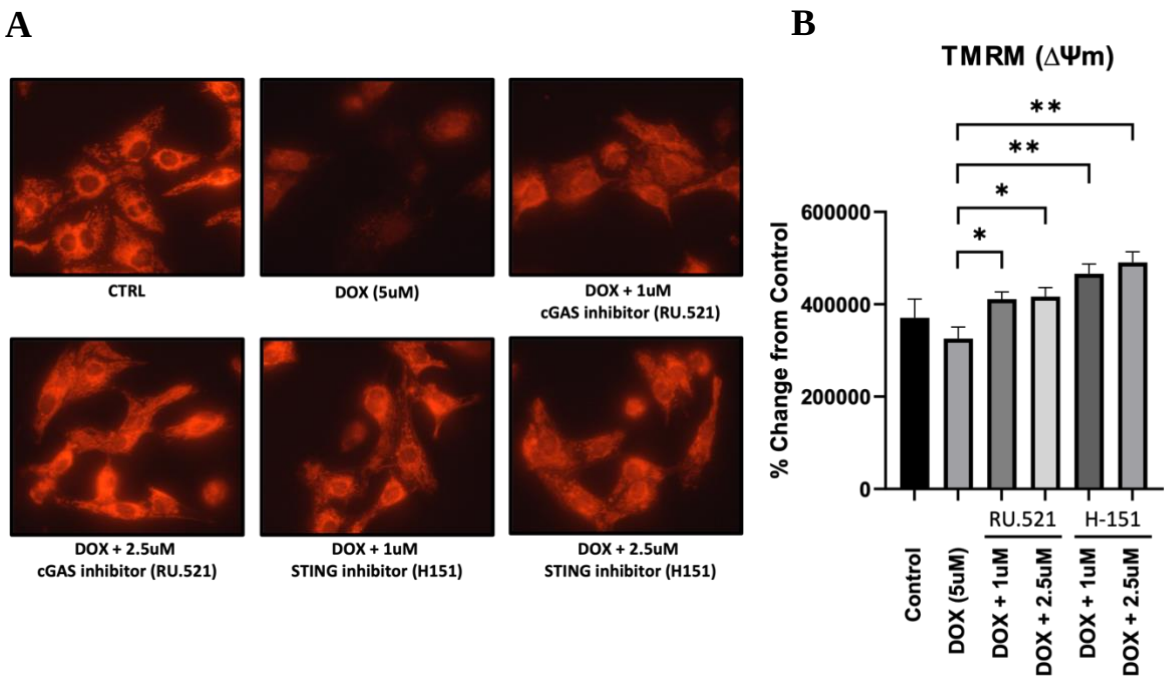


**Figure 5.3 cGAS and STING inhibition restores loss of Mitochondrial Membrane Potential (ΔΨm) induced by DOX in cardiac myocytes**

**Panel A.** Mitochondrial membrane potential (ΔΨm) was assessed using epifluorescence microscopy. Representative images of ventricular myocytes stained with TMRM (red) were taken for the treatment conditions: control (CTRL), doxorubicin (DOX), DOX with cGAS inhibitor RU.521 (1 µM and 2.5 µM), and DOX with STING inhibitor H-151 (1 µM and 2.5 µM). Diminished TMRM fluorescence indicates loss in ΔΨm.

**Panel B.** Quantitative analysis of ΔΨm. The histogram displays represents mean TMRM fluorescence intensity for each treatment condition, with the statistical significance is compared to the DOX-only condition: *P < 0.05 and **P < 0.01.

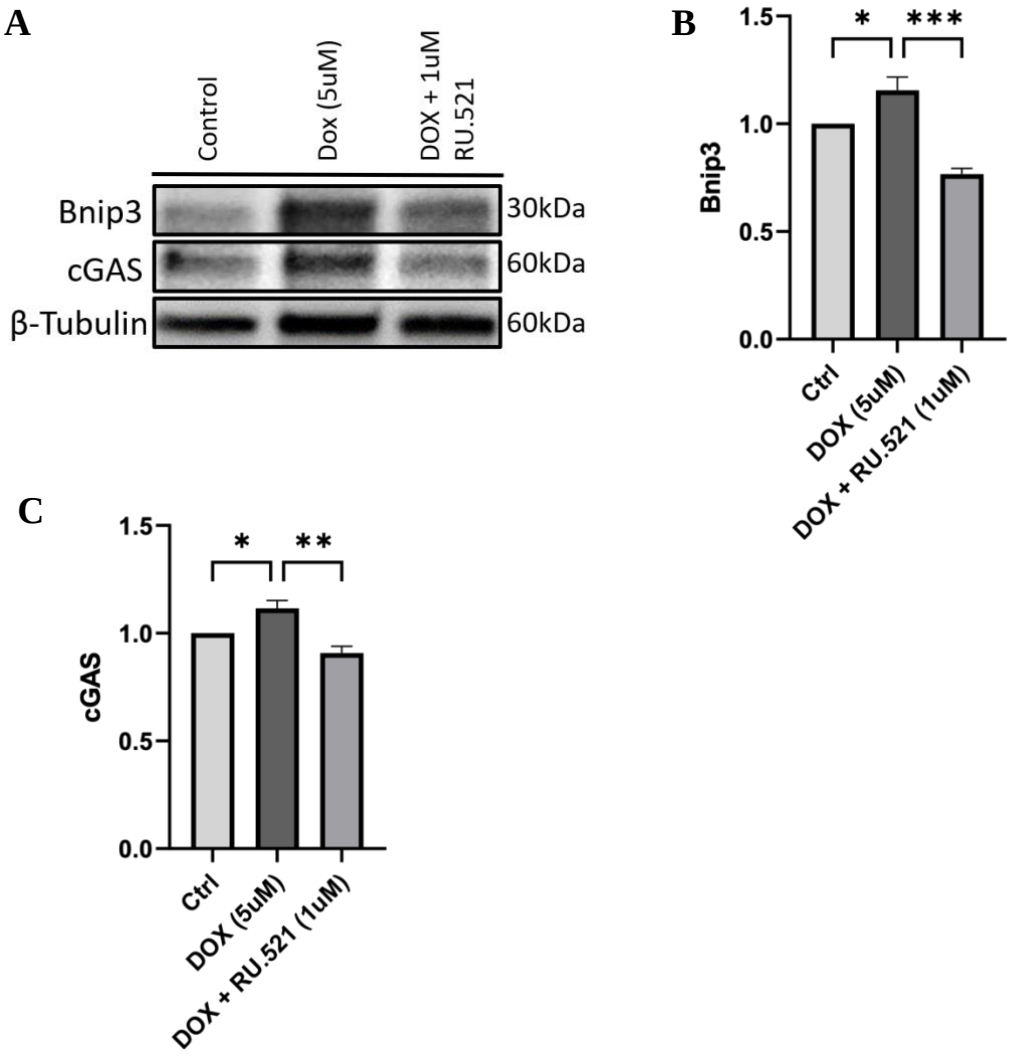


**Figure 5.4 cGAS inhibitor decreases the expresion of mitochondrial death protein Bnip3 induced by DOX**

**Panel A.** Western blot analysis depicting protein expression levels of cGAS and Bnip3 in ventricular myocytes under the following conditions: control (CTRL), doxorubicin (DOX, 5 µM), and DOX with cGAS inhibitor RU.521 (1 µM). The blot demonstrates that RU.521 treatment reduces Bnip3 expression induced by DOX.

**Panel B.** Quantitative analysis for protein expression from Panel A. Data are normalized to the control condition and presented as mean ± SEM. Statistical significance is indicated by *P < 0.05, **P < 0.01, and ***P < 0.001 compared to the DOX-only condition.

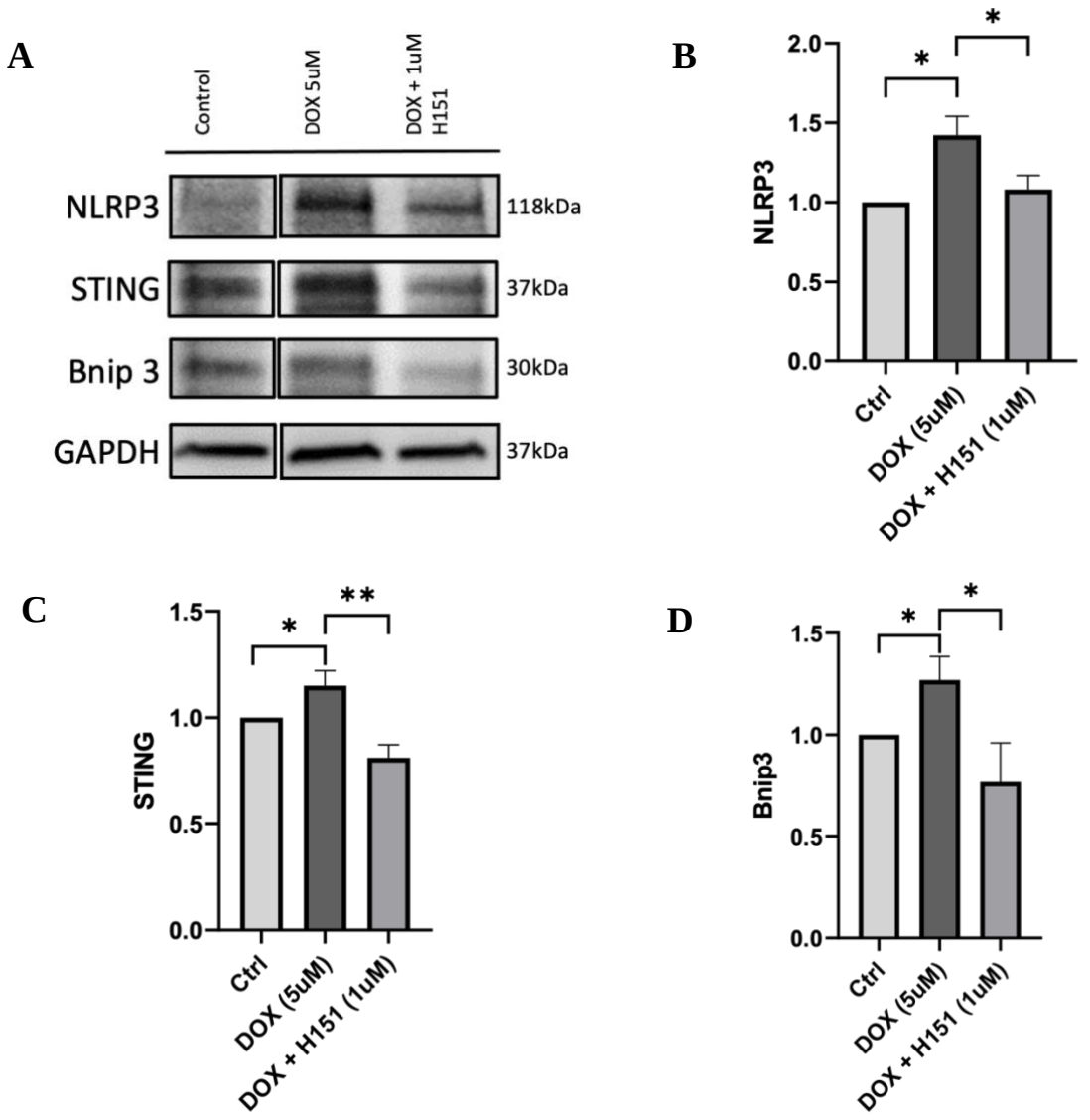


**Figure 5.5 STING inhibition mitigates DOX-induced expression of NLRP3 and Bnip3 in cardiac myocytes**

**Panel A.** Western blot analysis depicting protein levels of NLRP3, STING, and Bnip3 in ventricular myocytes under three conditions: control (CTRL), doxorubicin (DOX, 5 µM), and DOX with STING inhibitor H-151 (1 µM). The blot illustrates that H-151 treatment attenuates DOX-induced upregulation of NLRP3 and Bnip3.

**Panel B.** Quantitative analysis of protein expression from Panel A. Data are normalized to the control condition and presented as mean ± SEM. Asterisks denote statistical significance compared to the DOX-only condition: *P < 0.05, **P < 0.01, and ***P < 0.001.

## Discussion

Anthracycline drugs like Doxorubicin are highly potent against a broad spectrum of cancers. However, the cardiotoxic side of effect of DOX is a limiting factor for its clinical application (124,125). The cardiomyopathy induced by DOX is dose-dependent and presents as arrythmia, electrocardiogram (ECG) changes, reduction of left ventricular ejection fraction (LVEF) and severe cardiac dysfunction leading to heart failure (126). Heart failure is one of the leading causes of mortality, affecting millions of people worldwide (127,128). Cancer patients undergoing chemotherapy have a higher risk of developing heart failure due to the cardiotoxic effect of the treatment (129,130), with about 0.5-2.5% of cancer survivors progressing to end-stage heart failure (131). As such, there is no cure for heart failure, and therapies such as β-blockers and ACE inhibitors are symptomatic treatment strategies used to treat heart failure (126). While end-stage heart failure requires advance heart failure therapies such as heart transplantation (130,132). A complete understanding of the molecular mechanism associated with DOX-induced toxicity remains elusive. Consequently, there is still a significant demand for a deeper understanding of the fundamental mechanisms of anthracycline-induced cardiomyopathy, as well as the development of novel treatment approaches.

Intensive research suggests that DOX induces excessive oxidative stress, mitochondrial damage, inflammation, ultrastructural defects (myofibrillar loss and/or disarray) and cell death in cardiomyocytes (7,133,134). Furthermore, the cellular stress caused by DOX is known to cause DNA damage (135). DOX, being a topoisomerase IIβ inhibitor, induces DNA double-strand breaks (DSBs) production, selectively affecting oxidative phosphorylation, provoking ROS production and impairing mitochondrial biogenesis in cardiomyocytes, leading to cell death (136–138). Zhang et. al. showed that cardiomyocyte specific deletion of Top2b attenuated the DOX-induced cardiomyopathy (136). Mitochondrial DNA (mtDNA) damage

and mutation, along with elevated ROS production in the mitochondria, have been associated with DOX-induced mitochondrial damage and cardiotoxic pathogenies (139,140). The opening of the mitochondrial permeability transition pore in response to DOX treatment can allow the escape of mtDNA from mitochondria (141,142). The release of DNA from its compartments (nucleus and mitochondria) to the cytosol has been associated with cardiac inflammation, disorders, and heart failure (88,105,111,143). Additionally, previous research from our lab has established that DOX results in the loss of high mobility group box 1 (HMGB1) from the nucleus (7), suggesting that DOX-induced toxicity triggers the release of various danger-associated molecular patterns (DAMPs), thereby amplifying cellular stress responses in cardiac myocytes (85,122).

Cellular homeostasis is maintained by the autophagy process. It is responsible for the degrading and recycling of damaged organelles and cellular components (144). The precise relationship between autophagy and DOX remains to be fully elucidated, although accumulative evidence suggests that DOX disrupts the autophagy process (145). Studies have shown that DOX disrupts the proper completion of autophagy by hindering clearance of damaged cellular components (47,146–148). DOX impairs lysosomal acidification, hence blocking autophagic flux in cardiomyocytes (11). Dox reduces the formation of autophagolysosomes in the hearts of mice given DOX treatment (149). Consequently, impaired autophagy results in the accumulation of unprocessed autophagosomes and undegraded damaged cellular components such as mitochondria, promoting ROS overproduction and proteotoxicity, which further accelerate DOX-induced cardiac dysfunction (11,150).

A growing body of research suggests that the persistence of cytosolic DAMPs such as HMGB1 and DNA due to impaired autophagy can elicit an inflammatory response. The cGAS-STING innate immune pathway is responsible for detecting cellular DAMPs and is important for regulation of inflammatory responses (12). Its role in cardiovascular diseases like MI, atherosclerosis and heart failure has recently been identified (82,120). Notably, excessive inflammation has been reported in cancer patients and animal models that were treated with the DOX chemotherapy, signified by elevation in cytokine markers such as TNFa and IL-6 (9,151). Excessive inflammation (chronic or acute) in cancer patients is harmful as it can result in tissue damage, impaired left ventricular function and cardiomyocyte cell death (83).

In this study, we demonstrate convincing evidence that the cGAS-STING pathway is involved in DOX-induced cardiomyopathy. Herein, we show the activation of STING in the hearts of cancer patients who had suffered from heart failure following DOX treatment. We further confirmed our findings in neonatal cardiac myocytes. The interesting aspect of our study is that we found a dose-dependent increase in cGAS and STING protein expression. This finding correlated to the upregulation of the NLRP3 inflammasome. Therefore, indicating a direct link between DOX exposure and an inflammatory response.

An important feature of our study is that we show the presence of DNA in the cytosol of cardiomyocytes when exposed to DOX treatment. Live imaging showed that NucBlue dye, which produces blue florescence when bound to DNA, was confined to the nucleus under control condition. Strikingly, it was observed that DOX treatment led to the spillage of the blue staining into the cytoplasm. Furthermore, colocalization analysis and 3D imaging established that the GFP-LC3 puncta, which tags autophagosomes, engulfs the blue DNA staining. Our

findings suggest the induction of the autophagy process. However, literature suggests that under DOX disrupts the successful completion of autophagy (11,149). Hence, this leads us to conclude that the cytosolic DNA present in DOX-treated cells remain undegraded and can act as DAMPs. In addition to this, not all the DNA is enclosed by the autophagosome, making it possible for the cGAS to sense the DNA in the cytoplasm. Our study also revealed a reduction in the expression of DNase II protein, a lysosomal enzyme critical for the degradation of DNA (121). The decrease in expression of DNase II allows for the accumulated cytoplasmic DNA to persist, allowing it to activate of the innate cGAS-STING pathway.

Research has shown that HMGB1 promotes senescence in cancer cells via upregulation of STING (122). It has been previously established that HMGB-1, another DAMP, is released from the nucleus and contributes to cell death induced by DOX (7). From our current study we demonstrated that inhibition of HMGB1 can rescue cardiomyocytes from DOX-induced cell death. However, the relationship between HMGB1 and cGAS – STING signalling in DOX-induced cardiotoxicity needs more research.

Bnip3 is known to be involved in causing apoptotic cell death in cardiac myocytes when given DOX treatment. We show that the expression of the Bnip3 protein increases in a dose-dependent manner due to DOX. The activation of Bnip3 has been linked to mitochondrial defects induced by DOX (7). The same was observed as DOX treatment resulted in overproduction of ROS, mPTpore opening and loss of transmembrane potential in mitochondria. Furthermore, mtDNA leakage can occur if the mitochondria are damaged due to opening of PTpore in response to pathological stimulation (152). The leakage of mtDNA can then result in the activation of cGAS as it is a DNA sensor perpetuating a robust inflammatory

reaction and cardiac injury (141,142,152,153). In addition, DOX induced a high amount of cell death of cardiomyocytes.

A particularly intriguing aspect of our study is that cGAS-STING pathway inhibition mitigates DOX-induced mitochondrial dysfunction and cardiomyocyte death. Interestingly, our research showed that inhibiting either cGAS or STING using a pharmacological inhibitor suppresses the mitochondrial damage induced by DOX. Additionally, the cell death induced by DOX was significantly reduced using both cGAS (RU.521) and STING (H-151) inhibitor, respectively. The application of the inhibitor alongside DOX treatment suppressed excess production of ROS and opening of the mitochondrional permeability transition pore. As well as, the mitochondrial membrane potential loss was attenuated by the inhibitors. Our findings show that blocking cGAS and STING reduced the expression of the mitochondrial death protein Bnip3, which explains the reduction in mitochondrial dysfunction. The expression of the inflammasome NRLP3 was also suppressed using the STING inhibitor, blocking cardiac myocyte inflammation. These findings strongly indicate that DOX-induced mitochondrial and cardiac injury is mediated by the cGAS – STING signalling axis.

## Conclusion and Future Directions

In conclusion, our study provides novel mechanistic evidence that DOX-induced cardiotoxicity is mediated through the activation of the innate immune cGAS-STING pathway, resulting in inflammation, mitochondrial dysfunction and cell death. We show that The activation of this pathway upregulates Bnip3, exacerbating mitochondrial damage and cardiomyocyte apoptosis. Significantly, by inhibiting the cGAS – STING signalling, the mitochondrial perturbation induced by DOX and Bnip3 activation was mitigated. This study presents two potential therapeutic interventions: blocking cGAS or STING activity, which can ameliorate doxorubicin-induced cardiotoxicity. Therefore, adjuvant therapies that can target cGAS or STING can prove beneficial in preventing cardiomyopathy in cancer patients receiving DOX treatment and improving disease progression.

Moving forward, further research exploring the translational relevance of cGAS and STING inhibition in vivo models would help determine the implication and efficacy of the inhibitor in whole complex organisms. As mentioned before, investigating the effect of HMGB1 inhibition would deepen our understanding of the activation of the pathway. Our study highlights the importance of targeting the innate immune response as a promising mechanism to manage DOX-induced cardiotoxicity in cancer patients.

## References


1. Seddon B, Strauss SJ, Whelan J, Leahy M, Woll PJ, Cowie F, et al. Gemcitabine and docetaxel versus doxorubicin as first-line treatment in previously untreated advanced unresectable or metastatic soft-tissue sarcomas (GeDDiS): a randomised controlled phase 3 trial. Lancet Oncol. 2017 Oct;18(10):1397–410.

2. Jones IC, Dass CR. Doxorubicin-induced cardiotoxicity: causative factors and possible interventions. Vol. 74, The Journal of pharmacy and pharmacology. NLM (Medline); 2022. p. 1677–88.

3. Chatterjee K, Zhang J, Honbo N, Karliner JS. Doxorubicin cardiomyopathy. Vol. 115, Cardiology. 2010. p. 155–62.

4. Lotrionte M, Biondi-Zoccai G, Abbate A, Lanzetta G, D'Ascenzo F, Malavasi V, et al. Review and meta-analysis of incidence and clinical predictors of anthracycline cardiotoxicity. Am J Cardiol. 2013 Dec 15;112(12):1980–4.

5. Koleini N, Kardami E. Autophagy and mitophagy in the context of doxorubicin-induced cardiotoxicity [Internet]. Vol. 8, Oncotarget. 2017. Available from: www.impactjournals.com/oncotarget/

6. Sciarretta S, Maejima Y, Zablocki D, Sadoshima J. The Role of Autophagy in the Heart. The Annual Review of Physiology is online at [Internet]. 2018;80:1–26. Available from: https://doi.org/10.1146/annurev-physiol-021317-

7. Dhingra R, Margulets V, Chowdhury SR, Thliveris J, Jassal D, Fernyhough P, et al. Bnip3 mediates doxorubicin-induced cardiac myocyte necrosis and mortality through changes in mitochondrial signaling. Proc Natl Acad Sci U S A. 2014 Dec 23;111(51):E5537–44.

8. Shi S, Chen Y, Luo Z, Nie G, Dai Y. Role of oxidative stress and inflammation-related signaling pathways in doxorubicin-induced cardiomyopathy. Vol. 21, Cell Communication and Signaling. BioMed Central Ltd; 2023.

9. Dhingra R, Rabinovich-Nikitin I, Rothman S, Guberman M, Gang H, Margulets V, et al. Proteasomal Degradation of TRAF2 Mediates Mitochondrial Dysfunction in Doxorubicin-Cardiomyopathy. Circulation. 2022 Sep 20;146(12):934–54.

10. Kuno A, Hosoda R, Tsukamoto M, Sato T, Sakuragi H, Ajima N, et al. SIRT1 in the cardiomyocyte counteracts doxorubicin-induced cardiotoxicity via regulating histone H2AX. Cardiovasc Res. 2023 Jan 18;118(17):3360–73.

11. Li DL, Wang Z V, Ding G, Tan W, Luo X, Criollo A, et al. Doxorubicin Blocks Cardiomyocyte Autophagic Flux by Inhibiting Lysosome Acidification. Circulation. 2016 Apr 26;133(17):1668–87.

12. Li T, Chen ZJ. The cGAS-cGAMP-STI NG pathway connects DNA damage to inflammation, senescence, and cancer. Vol. 215, Journal of Experimental Medicine. Rockefeller University Press; 2018. p. 1287–99.

13. King KR, Aguirre AD, Ye YX, Sun Y, Roh JD, Ng RP, et al. IRF3 and type I interferons fuel a fatal response to myocardial infarction. Nat Med. 2017 Dec;23(12):1481–7.

14. Luo W, Wang Y, Zhang L, Ren P, Zhang C, Li Y, et al. Critical Role of Cytosolic DNA and Its Sensing Adaptor STING in Aortic Degeneration, Dissection, and Rupture. Circulation. 2020 Jan 7;141(1):42–66.

15. Sawicki KT, Sala V, Prever L, Hirsch E, Ardehali H, Ghigo A. Preventing and Treating Anthracycline Cardiotoxicity: New Insights. 2021; Available from: https://doi.org/10.1146/annurev-pharmtox-030620-

16. Arcamone F, Cassinelli G, Fantini G, Grein A, Orezzi P, Pol C, et al. Adriamycin, 14-hydroxydaunomycin, a new antitumor antibiotic from S. peucetius var. caesius. Biotechnol Bioeng. 1969 Nov;11(6):1101–10.

17. Young RC, Ozols RF, Myers CE. The anthracycline antineoplastic drugs. N Engl J Med [Internet]. 1981 Jul 16;305(3):139–53. Available from: http://www.ncbi.nlm.nih.gov/pubmed/7017406

18. Carvalho C, Santos RX, Cardoso S, Correia S, Oliveira PJ, Santos MS, et al. Doxorubicin: the good, the bad and the ugly effect. Curr Med Chem. 2009;16(25):3267–85.

19. Doxorubicin_PM_EN_265420_25-Nov-2022.

20. Bukowski K, Kciuk M, Kontek R. Mechanisms of Multidrug Resistance in Cancer Chemotherapy. Int J Mol Sci. 2020 May 2;21(9).

21. Swain SM, Whaley FS, Ewer MS. Congestive heart failure in patients treated with doxorubicin: a retrospective analysis of three trials. Cancer. 2003 Jun 1;97(11):2869–79.

22. Von Hoff DD, Layard MW, Basa P, Davis HL, Von Hoff AL, Rozencweig M, et al. Risk factors for doxorubicin-induced congestive heart failure. Ann Intern Med. 1979 Nov;91(5):710–7.

23. Chow EJ, Aggarwal S, Doody DR, Aplenc R, Armenian SH, Baker KS, et al. Dexrazoxane and Long-Term Heart Function in Survivors of Childhood Cancer. J Clin Oncol. 2023 Apr 20;41(12):2248–57.

24. Hellmann K. Preventing the cardiotoxicity of anthracyclines by dexrazoxane. BMJ. 1999 Oct 23;319(7217):1085–6.

25. Bansal N, Adams MJ, Ganatra S, Colan SD, Aggarwal S, Steiner R, et al. Strategies to prevent anthracycline-induced cardiotoxicity in cancer survivors. Cardiooncology. 2019;5:18.

26. Macedo AVS, Hajjar LA, Lyon AR, Nascimento BR, Putzu A, Rossi L, et al. Efficacy of Dexrazoxane in Preventing Anthracycline Cardiotoxicity in Breast Cancer. JACC CardioOncol. 2019 Sep;1(1):68–79.

27. Shaikh F, Dupuis LL, Alexander S, Gupta A, Mertens L, Nathan PC. Cardioprotection and Second Malignant Neoplasms Associated With Dexrazoxane in Children Receiving Anthracycline Chemotherapy: A Systematic Review and Meta-Analysis. J Natl Cancer Inst. 2016 Apr;108(4).

28. Tahover E, Segal A, Isacson R, Rosengarten O, Grenader T, Gips M, et al. Dexrazoxane added to doxorubicin-based adjuvant chemotherapy of breast cancer: a retrospective cohort study with a comparative analysis of toxicity and survival. Anticancer Drugs. 2017 Aug;28(7):787–94.

29. Goffart S, von Kleist-Retzow JC, Wiesner RJ. Regulation of mitochondrial proliferation in the heart: power-plant failure contributes to cardiac failure in hypertrophy. Cardiovasc Res. 2004 Nov 1;64(2):198–207.

30. Songbo M, Lang H, Xinyong C, Bin X, Ping Z, Liang S. Oxidative stress injury in doxorubicin-induced cardiotoxicity. Toxicol Lett. 2019 Jun 1;307:41–8.

31. Vitale R, Marzocco S, Popolo A. Role of Oxidative Stress and Inflammation in Doxorubicin-Induced Cardiotoxicity: A Brief Account. Int J Mol Sci. 2024 Jul 8;25(13).

32. Moris D, Spartalis M, Spartalis E, Karachaliou GS, Karaolanis GI, Tsourouflis G, et al. The role of reactive oxygen species in the pathophysiology of cardiovascular diseases and the clinical significance of myocardial redox. Ann Transl Med. 2017 Aug;5(16):326.

33. Cejas RB, Petrykey K, Sapkota Y, Burridge PW. Anthracycline Toxicity: Light at the End of the Tunnel? Annu Rev Pharmacol Toxicol. 2024 Jan 23;64:115–34.

34. Elfadadny A, Ragab RF, Hamada R, Al Jaouni SK, Fu J, Mousa SA, et al. Natural bioactive compounds-doxorubicin combinations targeting topoisomerase II-alpha: Anticancer efficacy and safety. Toxicol Appl Pharmacol. 2023 Feb 15;461:116405.

35. Eisner DA, Caldwell JL, Kistamás K, Trafford AW. Calcium and Excitation-Contraction Coupling in the Heart. Circ Res. 2017 Jul 7;121(2):181–95.

36. Shinlapawittayatorn K, Chattipakorn SC, Chattipakorn N. The effects of doxorubicin on cardiac calcium homeostasis and contractile function. J Cardiol. 2022 Aug;80(2):125–32.

37. Kim SY, Kim SJ, Kim BJ, Rah SY, Chung SM, Im MJ, et al. Doxorubicin-induced reactive oxygen species generation and intracellular Ca2+ increase are reciprocally modulated in rat cardiomyocytes. Exp Mol Med. 2006 Oct 31;38(5):535–45.

38. Donnarumma E, Kohlhaas M, Vimont E, Kornobis E, Chaze T, Gianetto QG, et al. Mitochondrial Fission Process 1 controls inner membrane integrity and protects against heart failure. Nat Commun. 2022 Nov 4;13(1):6634.

39. Brown DA, Perry JB, Allen ME, Sabbah HN, Stauffer BL, Shaikh SR, et al. Mitochondrial function as a therapeutic target in heart failure. Nat Rev Cardiol. 2017 Apr 22;14(4):238–50.

40. Gao F, Xu T, Zang F, Luo Y, Pan D. Cardiotoxicity of Anticancer Drugs: Molecular Mechanisms, Clinical Management and Innovative Treatment. Drug Des Devel Ther. 2024;18:4089–116.

41. Wu L, Wang L, Du Y, Zhang Y, Ren J. Mitochondrial quality control mechanisms as therapeutic targets in doxorubicin-induced cardiotoxicity. Trends Pharmacol Sci. 2023 Jan;44(1):34–49.

42. Chen R, Niu M, Hu X, He Y. Targeting mitochondrial dynamics proteins for the treatment of doxorubicin-induced cardiotoxicity. Front Mol Biosci. 2023;10:1241225.

43. Lebrecht D, Kirschner J, Geist A, Haberstroh J, Walker UA. Respiratory chain deficiency precedes the disrupted calcium homeostasis in chronic doxorubicin cardiomyopathy. Cardiovasc Pathol. 2010;19(5):e167-74.

44. Mitry MA, Edwards JG. Doxorubicin induced heart failure: Phenotype and molecular mechanisms. Int J Cardiol Heart Vasc. 2016 Mar;10:17–24.

45. Regula KM, Ens K, Kirshenbaum LA. Inducible expression of BNIP3 provokes mitochondrial defects and hypoxia-mediated cell death of ventricular myocytes. Circ Res. 2002 Aug 9;91(3):226–31.

46. Yin J, Guo J, Zhang Q, Cui L, Zhang L, Zhang T, et al. Doxorubicin-induced mitophagy and mitochondrial damage is associated with dysregulation of the PINK1/parkin pathway. Toxicol In Vitro. 2018 Sep;51:1–10.

47. Hoshino A, Mita Y, Okawa Y, Ariyoshi M, Iwai-Kanai E, Ueyama T, et al. Cytosolic p53 inhibits Parkin-mediated mitophagy and promotes mitochondrial dysfunction in the mouse heart. Nat Commun. 2013;4:2308.

48. Li A, Gao M, Jiang W, Qin Y, Gong G. Mitochondrial Dynamics in Adult Cardiomyocytes and Heart Diseases. Front Cell Dev Biol. 2020;8:584800.

49. Smirnova E, Griparic L, Shurland DL, van der Bliek AM. Dynamin-related protein Drp1 is required for mitochondrial division in mammalian cells. Mol Biol Cell. 2001 Aug;12(8):2245–56.

50. Guberman M, Dhingra R, Cross J, Margulets V, Gang H, Rabinovich-Nikitin I, et al. IKKβ stabilizes Mitofusin 2 and suppresses doxorubicin cardiomyopathy. Cardiovasc Res. 2024 Mar 13;120(2):164–73.

51. Chen R, Niu M, Hu X, He Y. Targeting mitochondrial dynamics proteins for the treatment of doxorubicin-induced cardiotoxicity. Front Mol Biosci. 2023;10:1241225.

52. Renu K, V G A, P B TP, Arunachalam S. Molecular mechanism of doxorubicin-induced cardiomyopathy - An update. Eur J Pharmacol. 2018 Jan 5;818:241–53.

53. Tai P, Chen X, Jia G, Chen G, Gong L, Cheng Y, et al. WGX50 mitigates doxorubicin-induced cardiotoxicity through inhibition of mitochondrial ROS and ferroptosis. J Transl Med. 2023 Nov 17;21(1):823.

54. Christidi E, Brunham LR. Regulated cell death pathways in doxorubicin-induced cardiotoxicity. Cell Death Dis. 2021 Apr 1;12(4):339.

55. Shi J, Abdelwahid E, Wei L. Apoptosis in Anthracycline Cardiomyopathy. Curr Pediatr Rev. 2011 Nov;7(4):329–36.

56. Reed JC. Bcl-2-family proteins and hematologic malignancies: history and future prospects. Blood. 2008 Apr 1;111(7):3322–30.

57. Christidi E, Brunham LR. Regulated cell death pathways in doxorubicin-induced cardiotoxicity. Cell Death Dis. 2021 Apr 1;12(4):339.

58. L'Ecuyer T, Sanjeev S, Thomas R, Novak R, Das L, Campbell W, et al. DNA damage is an early event in doxorubicin-induced cardiac myocyte death. Am J Physiol Heart Circ Physiol. 2006 Sep;291(3):H1273-80.

59. Kalivendi S V, Konorev EA, Cunningham S, Vanamala SK, Kaji EH, Joseph J, et al. Doxorubicin activates nuclear factor of activated T-lymphocytes and Fas ligand transcription: role of mitochondrial reactive oxygen species and calcium. Biochem J. 2005 Jul 15;389(Pt 2):527–39.

60. Sciarretta S, Maejima Y, Zablocki D, Sadoshima J. The Role of Autophagy in the Heart. Annu Rev Physiol. 2018 Feb 10;80:1–26.

61. Kciuk M, Gielecińska A, Mujwar S, Kołat D, Kałuzińska-Kołat Ż, Celik I, et al. Doxorubicin-An Agent with Multiple Mechanisms of Anticancer Activity. Cells. 2023 Feb 19;12(4).

62. Sishi BJN, Loos B, van Rooyen J, Engelbrecht AM. Autophagy upregulation promotes survival and attenuates doxorubicin-induced cardiotoxicity. Biochem Pharmacol. 2013 Jan 1;85(1):124–34.

63. Sun X, Meng H, Xiao J, Liu F, Du J, Zeng H. Pretreatment of 3-MA prevents doxorubicin-induced cardiotoxicity through inhibition of autophagy initiation. Toxicology. 2023 May 15;490:153512.

64. Dixon SJ, Lemberg KM, Lamprecht MR, Skouta R, Zaitsev EM, Gleason CE, et al. Ferroptosis: an iron-dependent form of nonapoptotic cell death. Cell. 2012 May 25;149(5):1060–72.

65. Abe K, Ikeda M, Ide T, Tadokoro T, Miyamoto HD, Furusawa S, et al. Doxorubicin causes ferroptosis and cardiotoxicity by intercalating into mitochondrial DNA and disrupting Alas1-dependent heme synthesis. Sci Signal. 2022 Nov;15(758):eabn8017.

66. Fang X, Wang H, Han D, Xie E, Yang X, Wei J, et al. Ferroptosis as a target for protection against cardiomyopathy. Proc Natl Acad Sci U S A. 2019 Feb 12;116(7):2672–80.

67. Wang Y, Yan S, Liu X, Deng F, Wang P, Yang L, et al. PRMT4 promotes ferroptosis to aggravate doxorubicin-induced cardiomyopathy via inhibition of the Nrf2/GPX4 pathway. Cell Death Differ. 2022 Oct;29(10):1982–95.

68. Bertheloot D, Latz E, Franklin BS. Necroptosis, pyroptosis and apoptosis: an intricate game of cell death. Cell Mol Immunol. 2021 May;18(5):1106–21.

69. Shi J, Zhao Y, Wang K, Shi X, Wang Y, Huang H, et al. Cleavage of GSDMD by inflammatory caspases determines pyroptotic cell death. Nature. 2015 Oct 29;526(7575):660–5.

70. Wang Y, Gao W, Shi X, Ding J, Liu W, He H, et al. Chemotherapy drugs induce pyroptosis through caspase-3 cleavage of a gasdermin. Nature. 2017 Jul 6;547(7661):99–103.

71. Zheng X, Zhong T, Ma Y, Wan X, Qin A, Yao B, et al. Bnip3 mediates doxorubicin-induced cardiomyocyte pyroptosis via caspase-3/GSDME. Life Sci. 2020 Feb 1;242:117186.

72. Zhang L, Jiang YH, Fan C, Zhang Q, Jiang YH, Li Y, et al. MCC950 attenuates doxorubicin-induced myocardial injury in vivo and in vitro by inhibiting NLRP3-mediated pyroptosis. Biomed Pharmacother. 2021 Nov;143:112133.

73. Zhang E, Shang C, Ma M, Zhang X, Liu Y, Song S, et al. Polyguluronic acid alleviates doxorubicin-induced cardiotoxicity by suppressing Peli1-NLRP3 inflammasome-mediated pyroptosis. Carbohydr Polym. 2023 Dec 1;321:121334.

74. Clayton ZS, Brunt VE, Hutton DA, Casso AG, Ziemba BP, Melov S, et al. Tumor Necrosis Factor Alpha-Mediated Inflammation and Remodeling of the Extracellular Matrix Underlies Aortic Stiffening Induced by the Common Chemotherapeutic Agent Doxorubicin. Hypertension. 2021 May 5;77(5):1581–90.

75. Sun L, Wu J, Du F, Chen X, Chen ZJ. Cyclic GMP-AMP synthase is a cytosolic DNA sensor that activates the type I interferon pathway. Science. 2013 Feb 15;339(6121):786–91.

76. Ablasser A, Goldeck M, Cavlar T, Deimling T, Witte G, Röhl I, et al. cGAS produces a 2’-5’-linked cyclic dinucleotide second messenger that activates STING. Nature. 2013 Jun 20;498(7454):380–4.

77. Burdette DL, Monroe KM, Sotelo-Troha K, Iwig JS, Eckert B, Hyodo M, et al. STING is a direct innate immune sensor of cyclic di-GMP. Nature. 2011 Sep 25;478(7370):515–8.

78. Ishikawa H, Barber GN. STING is an endoplasmic reticulum adaptor that facilitates innate immune signalling. Nature. 2008 Oct 2;455(7213):674–8.

79. Hopfner KP, Hornung V. Molecular mechanisms and cellular functions of cGAS-STING signalling. Nat Rev Mol Cell Biol. 2020 Sep;21(9):501–21.

80. Kim J, Kim HS, Chung JH. Molecular mechanisms of mitochondrial DNA release and activation of the cGAS-STING pathway. Exp Mol Med. 2023 Mar;55(3):510–9.

81. Hu MM, Shu HB. Innate Immune Response to Cytoplasmic DNA: Mechanisms and Diseases. Annu Rev Immunol. 2020 Apr 26;38:79–98.

82. Du Y, Zhang H, Nie X, Qi Y, Shi S, Han Y, et al. Link between sterile inflammation and cardiovascular diseases: Focus on cGAS-STING pathway in the pathogenesis and therapeutic prospect. Front Cardiovasc Med. 2022;9:965726.

83. Oduro PK, Zheng X, Wei J, Yang Y, Wang Y, Zhang H, et al. The cGAS-STING signaling in cardiovascular and metabolic diseases: Future novel target option for pharmacotherapy. Acta Pharm Sin B. 2022 Jan;12(1):50–75.

84. Chen GY, Nuñez G. Sterile inflammation: sensing and reacting to damage. Nat Rev Immunol. 2010 Dec;10(12):826–37.

85. Gong T, Liu L, Jiang W, Zhou R. DAMP-sensing receptors in sterile inflammation and inflammatory diseases. Nat Rev Immunol. 2020 Feb;20(2):95–112.

86. Ding HS, Huang Y, Qu JF, Wang YJ, Huang ZY, Wang FY, et al. Panaxynol ameliorates cardiac ischemia/reperfusion injury by suppressing NLRP3-induced pyroptosis and apoptosis via HMGB1/TLR4/NF-κB axis. Int Immunopharmacol. 2023 Aug;121:110222.

87. Li X, Shu C, Yi G, Chaton CT, Shelton CL, Diao J, et al. Cyclic GMP-AMP synthase is activated by double-stranded DNA-induced oligomerization. Immunity. 2013 Dec 12;39(6):1019–31.

88. Zhang X, Wu J, Du F, Xu H, Sun L, Chen Z, et al. The cytosolic DNA sensor cGAS forms an oligomeric complex with DNA and undergoes switch-like conformational changes in the activation loop. Cell Rep. 2014 Feb 13;6(3):421–30.

89. Zhang X, Shi H, Wu J, Zhang X, Sun L, Chen C, et al. Cyclic GMP-AMP containing mixed phosphodiester linkages is an endogenous high-affinity ligand for STING. Mol Cell. 2013 Jul 25;51(2):226–35.

90. Shang G, Zhu D, Li N, Zhang J, Zhu C, Lu D, et al. Crystal structures of STING protein reveal basis for recognition of cyclic di-GMP. Nat Struct Mol Biol. 2012 Jun 24;19(7):725–7.

91. Saitoh T, Fujita N, Hayashi T, Takahara K, Satoh T, Lee H, et al. Atg9a controls dsDNA-driven dynamic translocation of STING and the innate immune response. Proc Natl Acad Sci U S A. 2009 Dec 8;106(49):20842–6.

92. Tanaka Y, Chen ZJ. STING specifies IRF3 phosphorylation by TBK1 in the cytosolic DNA signaling pathway. Sci Signal. 2012 Mar 6;5(214):ra20.

93. Yang NSY, Zhong WJ, Sha HX, Zhang CY, Jin L, Duan JX, et al. mtDNA-cGAS-STING axis-dependent NLRP3 inflammasome activation contributes to postoperative cognitive dysfunction induced by sevoflurane in mice. Int J Biol Sci. 2024;20(5):1927–46.

94. Eming SA, Wynn TA, Martin P. Inflammation and metabolism in tissue repair and regeneration. Science. 2017 Jun 9;356(6342):1026–30.

95. Decout A, Katz JD, Venkatraman S, Ablasser A. The cGAS-STING pathway as a therapeutic target in inflammatory diseases. Nat Rev Immunol. 2021 Sep;21(9):548–69.

96. Lee-Kirsch MA, Gong M, Chowdhury D, Senenko L, Engel K, Lee YA, et al. Mutations in the gene encoding the 3’-5’ DNA exonuclease TREX1 are associated with systemic lupus erythematosus. Nat Genet. 2007 Sep;39(9):1065–7.

97. Gray EE, Treuting PM, Woodward JJ, Stetson DB. Cutting Edge: cGAS Is Required for Lethal Autoimmune Disease in the Trex1-Deficient Mouse Model of Aicardi-Goutières Syndrome. J Immunol. 2015 Sep 1;195(5):1939–43.

98. Hagiwara AM, Moore RE, Wallace DJ, Ishimori M, Jefferies CA. Regulation of cGAS-STING Pathway - Implications for Systemic Lupus Erythematosus. Rheumatology and immunology research. 2021 Sep;2(3):173–84.

99. Grieves JL, Fye JM, Harvey S, Grayson JM, Hollis T, Perrino FW. Exonuclease TREX1 degrades double-stranded DNA to prevent spontaneous lupus-like inflammatory disease. Proc Natl Acad Sci U S A. 2015 Apr 21;112(16):5117–22.

100. Li T, Yum S, Wu J, Li M, Deng Y, Sun L, et al. cGAS activation in classical dendritic cells causes autoimmunity in TREX1-deficient mice. Proc Natl Acad Sci U S A. 2024 Sep 17;121(38):e2411747121.

101. Wang J, Li R, Lin H, Qiu Q, Lao M, Zeng S, et al. Accumulation of cytosolic dsDNA contributes to fibroblast-like synoviocytes-mediated rheumatoid arthritis synovial inflammation. Int Immunopharmacol. 2019 Nov;76:105791.

102. Gao D, Li T, Li XD, Chen X, Li QZ, Wight-Carter M, et al. Activation of cyclic GMP-AMP synthase by self-DNA causes autoimmune diseases. Proc Natl Acad Sci U S A. 2015 Oct 20;112(42):E5699-705.

103. Bakhoum SF, Ngo B, Laughney AM, Cavallo JA, Murphy CJ, Ly P, et al. Chromosomal instability drives metastasis through a cytosolic DNA response. Nature. 2018 Jan 25;553(7689):467–72.

104. Abdullah A, Zhang M, Frugier T, Bedoui S, Taylor JM, Crack PJ. STING-mediated type-I interferons contribute to the neuroinflammatory process and detrimental effects following traumatic brain injury. J Neuroinflammation. 2018 Nov 21;15(1):323.

105. Yan M, Li Y, Luo Q, Zeng W, Shao X, Li L, et al. Mitochondrial damage and activation of the cytosolic DNA sensor cGAS-STING pathway lead to cardiac pyroptosis and hypertrophy in diabetic cardiomyopathy mice. Cell Death Discov. 2022 May 11;8(1):258.

106. Manolis AS, Manolis AA, Manolis TA, Apostolaki NE, Apostolopoulos EJ, Melita H, et al. Mitochondrial dysfunction in cardiovascular disease: Current status of translational research/clinical and therapeutic implications. Med Res Rev. 2021 Jan;41(1):275–313.

107. Pham PT, Fukuda D, Nishimoto S, Kim-Kaneyama JR, Lei XF, Takahashi Y, et al. STING, a cytosolic DNA sensor, plays a critical role in atherogenesis: a link between innate immunity and chronic inflammation caused by lifestyle-related diseases. Eur Heart J. 2021 Nov 7;42(42):4336–48.

108. Frostegård J. Immunity, atherosclerosis and cardiovascular disease. BMC Med. 2013 Dec 1;11(1):117.

109. Frangogiannis NG. Regulation of the inflammatory response in cardiac repair. Circ Res. 2012 Jan 6;110(1):159–73.

110. King KR, Aguirre AD, Ye YX, Sun Y, Roh JD, Ng RP, et al. IRF3 and type I interferons fuel a fatal response to myocardial infarction. Nat Med. 2017 Dec;23(12):1481–7.

111. Cao DJ, Schiattarella GG, Villalobos E, Jiang N, May HI, Li T, et al. Cytosolic DNA Sensing Promotes Macrophage Transformation and Governs Myocardial Ischemic Injury. Circulation. 2018 Jun 12;137(24):2613–34.

112. Ter Horst EN, Krijnen PAJ, Hakimzadeh N, Robbers LFHJ, Hirsch A, Nijveldt R, et al. Elevated monocyte-specific type I interferon signalling correlates positively with cardiac healing in myocardial infarct patients but interferon alpha application deteriorates myocardial healing in rats. Basic Res Cardiol. 2018 Nov 12;114(1):1.

113. Hu S, Gao Y, Gao R, Wang Y, Qu Y, Yang J, et al. The selective STING inhibitor H-151 preserves myocardial function and ameliorates cardiac fibrosis in murine myocardial infarction. Int Immunopharmacol. 2022 Jun;107:108658.

114. Liu H, Yang P, Chen S, Wang S, Jiang L, Xiao X, et al. Ncf1 knockout in smooth muscle cells exacerbates angiotensin II-induced aortic aneurysm and dissection by activating the STING pathway. Cardiovasc Res. 2024 Jul 31;120(9):1081–96.

115. Morita M, Stamp G, Robins P, Dulic A, Rosewell I, Hrivnak G, et al. Gene-targeted mice lacking the Trex1 (DNase III) 3'-->5' DNA exonuclease develop inflammatory myocarditis. Mol Cell Biol. 2004 Aug;24(15):6719–27.

116. Pham PT, Fukuda D, Nishimoto S, Kim-Kaneyama JR, Lei XF, Takahashi Y, et al. STING, a cytosolic DNA sensor, plays a critical role in atherogenesis: a link between innate immunity and chronic inflammation caused by lifestyle-related diseases. Eur Heart J. 2021 Nov 7;42(42):4336–48.

117. Li X, Chen X, Zheng L, Chen M, Zhang Y, Zhu R, et al. Non-canonical STING-PERK pathway dependent epigenetic regulation of vascular endothelial dysfunction via integrating IRF3 and NF-κB in inflammatory response. Acta Pharm Sin B. 2023 Dec;13(12):4765–84.

118. Yarmohammadi F, Karbasforooshan H, Hayes AW, Karimi G. Inflammation suppression in doxorubicin-induced cardiotoxicity: natural compounds as therapeutic options. Naunyn Schmiedebergs Arch Pharmacol. 2021 Oct;394(10):2003–11.

119. Wang L, Chen Q, Qi H, Wang C, Wang C, Zhang J, et al. Doxorubicin-Induced Systemic Inflammation Is Driven by Upregulation of Toll-Like Receptor TLR4 and Endotoxin Leakage. Cancer Res. 2016 Nov 15;76(22):6631–42.

120. An C, Li Z, Chen Y, Huang S, Yang F, Hu Y, et al. The cGAS-STING pathway in cardiovascular diseases: from basic research to clinical perspectives. Cell Biosci. 2024 May 8;14(1):58.

121. Zhuang J, Du X, Liu K, Hao J, Wang H, An R, et al. DNase II Can Efficiently Digest RNA and Needs to Be Redefined as a Nuclease. Cells. 2024 Sep 11;13(18).

122. Lee JJ, Park IH, Kwak MS, Rhee WJ, Kim SH, Shin JS. HMGB1 orchestrates STING-mediated senescence via TRIM30α modulation in cancer cells. Cell Death Discov. 2021 Feb 8;7(1):28.

123. Zhang J, Ney PA. Role of BNIP3 and NIX in cell death, autophagy, and mitophagy. Cell Death Differ. 2009 Jul;16(7):939–46.

124. Herrmann J. Adverse cardiac effects of cancer therapies: cardiotoxicity and arrhythmia. Nat Rev Cardiol. 2020 Aug;17(8):474–502.

125. Carvalho C, Santos RX, Cardoso S, Correia S, Oliveira PJ, Santos MS, et al. Doxorubicin: the good, the bad and the ugly effect. Curr Med Chem. 2009;16(25):3267–85.

126. Herrmann J, Lerman A, Sandhu NP, Villarraga HR, Mulvagh SL, Kohli M. Evaluation and management of patients with heart disease and cancer: cardio-oncology. Mayo Clin Proc. 2014 Sep;89(9):1287–306.

127. Savarese G, Becher PM, Lund LH, Seferovic P, Rosano GMC, Coats AJS. Global burden of heart failure: a comprehensive and updated review of epidemiology. Cardiovasc Res. 2023 Jan 18;118(17):3272–87.

128. Martin SS, Aday AW, Almarzooq ZI, Anderson CAM, Arora P, Avery CL, et al. 2024 Heart Disease and Stroke Statistics: A Report of US and Global Data From the American Heart Association. Circulation. 2024 Feb 20;149(8):e347–913.

129. Nadruz W, West E, Sengeløv M, Grove GL, Santos M, Groarke JD, et al. Cardiovascular phenotype and prognosis of patients with heart failure induced by cancer therapy. Heart. 2019 Jan;105(1):34–41.

130. Lenneman AJ, Wang L, Wigger M, Frangoul H, Harrell FE, Silverstein C, et al. Heart transplant survival outcomes for adriamycin-dilated cardiomyopathy. Am J Cardiol. 2013 Feb 15;111(4):609–12.

131. Oliveira GH, Qattan MY, Al-Kindi S, Park SJ. Advanced heart failure therapies for patients with chemotherapy-induced cardiomyopathy. Circ Heart Fail. 2014 Nov;7(6):1050–8.

132. Araujo-Gutierrez R, Ibarra-Cortez SH, Estep JD, Bhimaraj A, Guha A, Hussain I, et al. Incidence and outcomes of cancer treatment-related cardiomyopathy among referrals for advanced heart failure. Cardiooncology. 2018;4:3.

133. Min K, Kwon OS, Smuder AJ, Wiggs MP, Sollanek KJ, Christou DD, et al. Increased mitochondrial emission of reactive oxygen species and calpain activation are required for doxorubicin-induced cardiac and skeletal muscle myopathy. J Physiol. 2015 Apr 15;593(8):2017–36.

134. Bi Y, Xu H, Wang X, Zhu H, Ge J, Ren J, et al. FUNDC1 protects against doxorubicin-induced cardiomyocyte PANoptosis through stabilizing mtDNA via interaction with TUFM. Cell Death Dis. 2022 Dec 5;13(12):1020.

135. Xiao B, Hong L, Cai X, Mei S, Zhang P, Shao L. The true colors of autophagy in doxorubicin-induced cardiotoxicity. Oncol Lett. 2019 Sep;18(3):2165–72.

136. Zhang S, Liu X, Bawa-Khalfe T, Lu LS, Lyu YL, Liu LF, et al. Identification of the molecular basis of doxorubicin-induced cardiotoxicity. Nat Med. 2012 Nov;18(11):1639–42.

137. Pommier Y, Leo E, Zhang H, Marchand C. DNA topoisomerases and their poisoning by anticancer and antibacterial drugs. Chem Biol. 2010 May 28;17(5):421–33.

138. Vejpongsa P, Yeh ETH. Topoisomerase 2β: a promising molecular target for primary prevention of anthracycline-induced cardiotoxicity. Clin Pharmacol Ther. 2014 Jan;95(1):45–52.

139. Lebrecht D, Kokkori A, Ketelsen UP, Setzer B, Walker UA. Tissue-specific mtDNA lesions and radical-associated mitochondrial dysfunction in human hearts exposed to doxorubicin. J Pathol. 2005 Dec;207(4):436–44.

140. Lebrecht D, Setzer B, Ketelsen UP, Haberstroh J, Walker UA. Time-dependent and tissue-specific accumulation of mtDNA and respiratory chain defects in chronic doxorubicin cardiomyopathy. Circulation. 2003 Nov 11;108(19):2423–9.

141. Zhang W, Li G, Luo R, Lei J, Song Y, Wang B, et al. Cytosolic escape of mitochondrial DNA triggers cGAS-STING-NLRP3 axis-dependent nucleus pulposus cell pyroptosis. Exp Mol Med. 2022 Feb;54(2):129–42.

142. Wei K, Chen T, Fang H, Shen X, Tang Z, Zhao J. Mitochondrial DNA release via the mitochondrial permeability transition pore activates the cGAS-STING pathway, exacerbating inflammation in acute Kawasaki disease. Cell Commun Signal. 2024 Jun 13;22(1):328.

143. Guo Y, You Y, Shang FF, Wang X, Huang B, Zhao B, et al. iNOS aggravates pressure overload-induced cardiac dysfunction via activation of the cytosolic-mtDNA-mediated cGAS-STING pathway. Theranostics. 2023;13(12):4229–46.

144. Hansen M, Rubinsztein DC, Walker DW. Autophagy as a promoter of longevity: insights from model organisms. Nat Rev Mol Cell Biol. 2018 Sep;19(9):579–93.

145. Bartlett JJ, Trivedi PC, Pulinilkunnil T. Autophagic dysregulation in doxorubicin cardiomyopathy. J Mol Cell Cardiol. 2017 Mar;104:1–8.

146. Wang Y, Lu X, Wang X, Qiu Q, Zhu P, Ma L, et al. atg7-Based Autophagy Activation Reverses Doxorubicin-Induced Cardiotoxicity. Circ Res. 2021 Oct;129(8):e166–82.

147. Yoshida M, Shiojima I, Ikeda H, Komuro I. Chronic doxorubicin cardiotoxicity is mediated by oxidative DNA damage-ATM-p53-apoptosis pathway and attenuated by pitavastatin through the inhibition of Rac1 activity. J Mol Cell Cardiol. 2009 Nov;47(5):698–705.

148. Chang YL, Lee HJ, Liu ST, Lin YS, Chen TC, Hsieh TY, et al. Different roles of p53 in the regulation of DNA damage caused by 1,2-heteroannelated anthraquinones and doxorubicin. Int J Biochem Cell Biol. 2011 Dec;43(12):1720–8.

149. Xu X, Bucala R, Ren J. Macrophage migration inhibitory factor deficiency augments doxorubicin-induced cardiomyopathy. J Am Heart Assoc. 2013 Dec 12;2(6):e000439.

150. Koleini N, Kardami E. Autophagy and mitophagy in the context of doxorubicin-induced cardiotoxicity. Oncotarget. 2017 Jul 11;8(28):46663–80.

151. Hutchins E, Yang EH, Stein-Merlob AF. Inflammation in Chemotherapy-Induced Cardiotoxicity. Curr Cardiol Rep. 2024 Dec;26(12):1329–40.

152. Guo Y, Gu R, Gan D, Hu F, Li G, Xu G. Mitochondrial DNA drives noncanonical inflammation activation via cGAS-STING signaling pathway in retinal microvascular endothelial cells. Cell Commun Signal. 2020 Oct 28;18(1):172.

153. Zhou L, Zhang YF, Yang FH, Mao HQ, Chen Z, Zhang L. Mitochondrial DNA leakage induces odontoblast inflammation via the cGAS-STING pathway. Cell Commun Signal. 2021 May 20;19(1):58.